CLIMATE CHANGE IMPACTS ON THE HYDROLOGY OF THE GREAT LAKES BASIN AND SOCIETAL IMPLICATIONS

By

Phyllis Feldpausch

A THESIS

Submitted to
Michigan State University
in partial fulfillment of the requirements
for the degree of

Environmental Engineering—Master of Science

2024

ABSTRACT

The Great Lakes Basin (GLB) in North America is home to over 30 million inhabitants and contributes more than 6 trillion dollars to the US GDP annually. Of which, 20% is generated from agriculture, making it the 2nd largest primary sector in the region's economy. Thus, understanding the long-term impacts of climate change on the GLB hydrology is crucial for ensuring the well-being of its people, economy, and environment. In this study, I investigate the impacts of climate change on the hydrodynamics of the GLB by analyzing (1) historical data and (2) projected future conditions. The CaMa-Flood model, a high-resolution (5km with flood attributes downscaled to 90m) hydrodynamics model, is forced by combinations of different hydrological and global climate models from various sources to simulate future conditions under 3 socioeconomic development pathways, combinations of Representative Concentration Pathways and Shared Socioeconomic Pathways (RCP 2.6-SSP1, RCP 4.5-SSP3 and RCP 8.5-SSP5) over an 85-year period (2015-2100). Historically observed data from 254 USGS stream gauge stations showed that 87.8% showed an increasing trend in water volume over the past 25 years, which has been linked to changes in precipitation, snow-melt timing, and increased magnitude and frequency of hydrological extremes including floods and droughts. Simulation results suggest that this trend is likely to continue into the future. First, substantial changes are expected in the seasonal hydrologic regime throughout the GLB, especially a major shift in the timing of peak flows from spring to winter, by up to a month in some areas by the end of the 21st century. Furthermore, results also suggest an overall increase in water balance, indicated by an increase in mean surface water storage by up to 20% in some areas. This is also reflected by an increase in lake water levels. Moreover, the frequency of extreme floods increases by 400-2000% under all climate change scenarios by the late century, especially SSP3 and SSP5. This study provides a comprehensive analysis on the impacts of climate change on the hydrology of the GLB, allowing for the anticipation and design prevention of future devastating hydrological events.

ACKNOWLEDGEMENTS

Special thank you to my advisor, Dr. Yadu Pokhrel, for unending support and invaluable patience, feedback and kindness. I never would have been able to complete my Masters' Degree without him. Thank you to Mr. Huy Dang, my graduate student mentor, and all of my friends and lab mates for feedback and support. I also could not have completed this journey without the knowledge and feedback of my committee members, Dr. Shu-Guang Li and Dr. Phanikumar Mantha.

This would not have been possible without the generous support of the Rose Graduate Fellowship in Water Research, and the Clifford Humphrys Fellowship for Preservation of Water Quality in the Great Lakes. Additionally, I acknowledge funding from the National Science Foundation (Award: 1752729).

Lastly, I would be remiss in not mentioning my friends and my family, especially my sister, Morgan, for their endless encouragement and support. In particular, I would like to thank my sister for always picking up the phone when I needed her to. I would also like to thank my cat, Bosco, for his delightful companionship.

TABLE OF CONTENTS

LIST OF TABLES

LIST OF FIGURES

CHAPTER 1

INTRODUCTION

1.1 Background

Climate change presents severe challenges globally, leading to devastating floods and droughts, impacting water availability, infrastructure and agriculture (IPCC Report) [18, 60]. Understanding these consequences is vital for water security and sustainable food production [53, 71, 85, 60].

The Great Lakes Basin (GLB), spanning over 520,000 km^2, is home to five of the world's largest freshwater lakes connected by 5,000 rivers and tributaries, holding a fifth of all global fresh surface water [33]. It is also a population hub and an economic powerhouse: home to a quarter of all Canadian citizens and 10% of all Americans, a total of more than 30 million people who generate over $3 trillion in gross domestic product while employing nearly 26 million people and making $1 trillion in wages annually [29]. More than 8% of US total agricultural products (worth of $15 billion) is cultivated in the GLB across more than 130,000 km^2 of farms [19].

Under climate change, this region faces unprecedented climatic shifts including temperature increases and variable precipitation patterns, which are likely to adversely impact its agricultural landscape and hydrological dynamics. Average annual temperature is predicted to increase throughout the basin, by up to 1-3° C by mid-century and up to 6.5°C by 2100 [10, 17]. On the contrary, projected changes in precipitation under climate change in the GLB vary greatly both spatially and temporally [85]. Most recent studies have quantified a significant increase in winter and spring precipitation and a significant decrease in the summer [16, 17, 20, 80]. Furthermore, increases in high flow and decreases in low flows point to increasing intensity of extreme hydrological events [20, 26]. However, some studies anticipate an overall increase [26, 68]. or decrease [22, 69] in total annual precipitation, rather than a change in timing and magnitude. Others have found consistent patterns in streamflow and precipitation changes spatially [44].

Seasonal streamflow characteristics in the GLB include a distinct wet and dry season pattern, with the wet season spanning approximately February to May, and the dry season June to September [11, 84]. Peak flows in this region are caused by a combination of heavy spring precipitation and

snowmelt due to higher temperatures [16]. Recent studies project a shift in peak flow timing by up to a month by the end of the century, increases in high flows and decreases in low flows [16, 17, 86]. Further, summer river discharge is reflected by lower rates of precipitation. Hydrological drought can be measured and analyzed using a streamflow drought index (SDI) [86]. Summer droughts are common in the GLB, however they have intensified in recent years, and this pattern is projected to continue [7]. It is crucial to understand spatial and temporal distributions for these changes in the timing and magnitude of hydrological events in the region to uncover the implications for water availability.

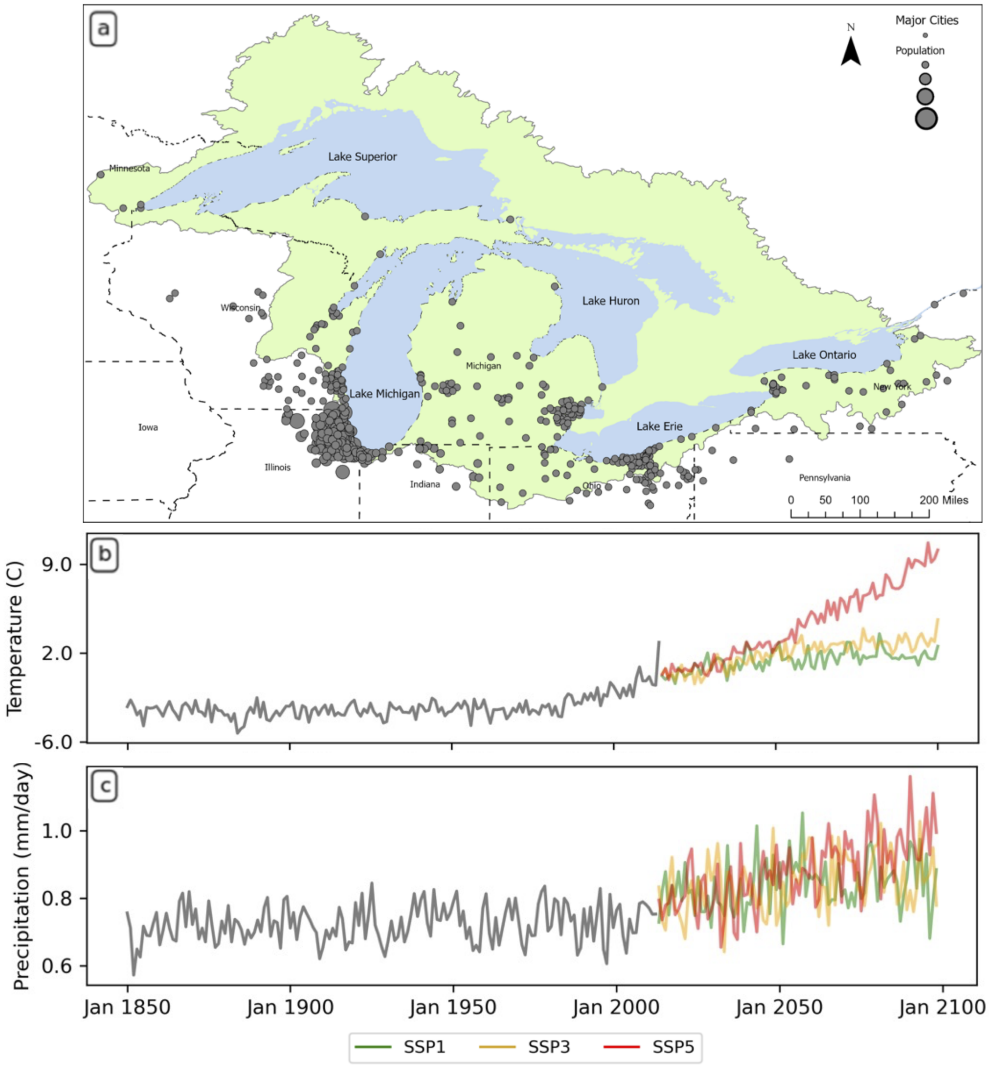

Figure 1.1 Great Lakes Basin map, annual temperature and precipitation.

Figure 1.1a shows the GLB, highlighting major cities and populated areas, whereas Figure 1.1b and Figure 1.1c show historical and projected annual average temperature and precipitation, respectively, under three climate change scenarios.

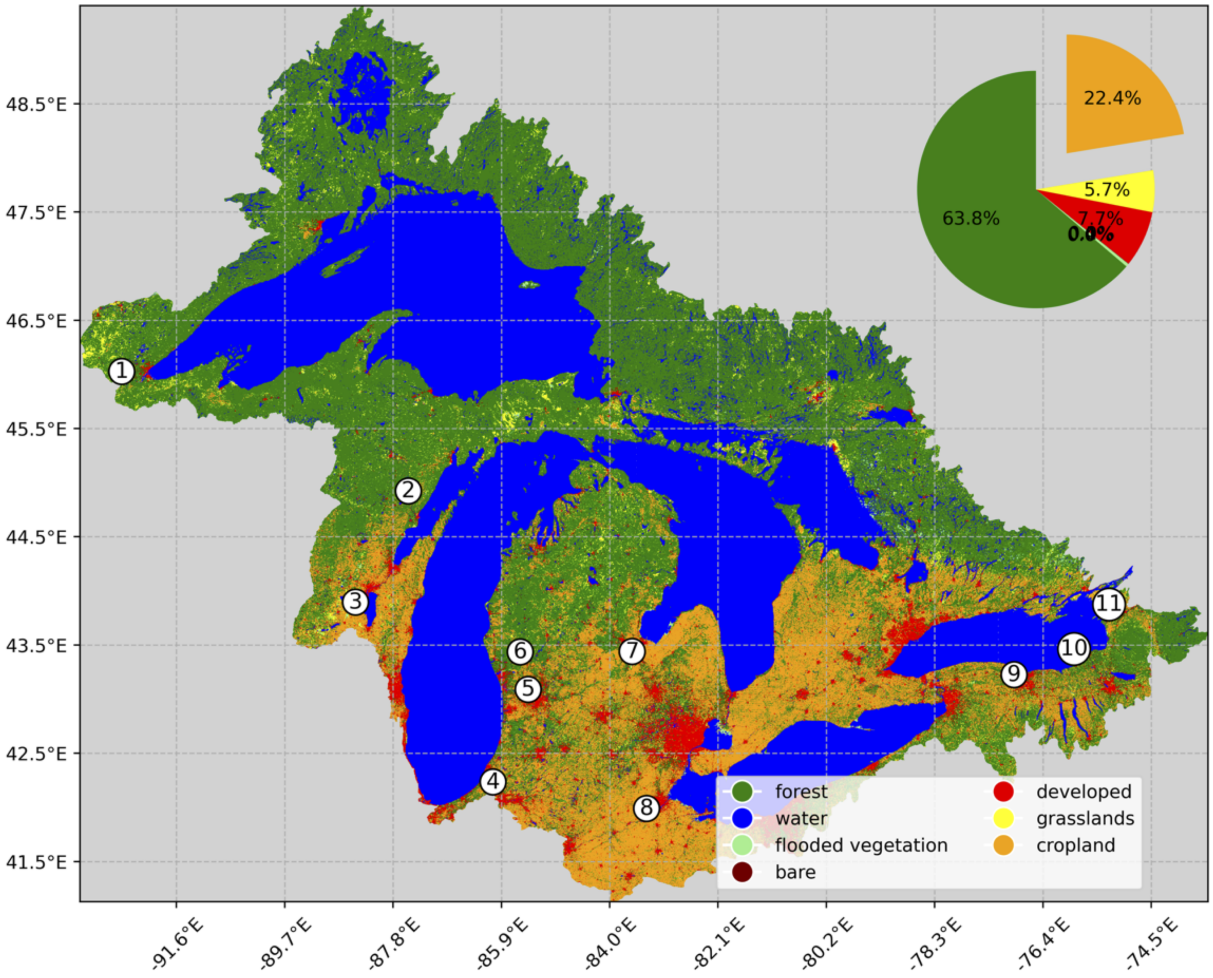

Figure 1.2 Great Lakes Basin land use/land cover map.

Figure 1.2 shows the basin domain and the major land cover types from remotely sensed data [46]. Agriculture dominates the southern portion of the basin, including Southern Michigan, Northern Ohio, and Southwestern Ontario, occupying nearly a quarter of the land in the GLB [50].

1.1.1 Agriculture

Rising temperatures and changing precipitation patterns can lead to more frequent and intense droughts, heatwaves, and extreme weather events, the exacerbation of such extreme events and shifts in seasonal timing would directly affect crop yield and ultimately food security [1, 58, 57]. Previous studies predicted a 20-40% decrease in corn yield across the United States by 2050 due to these changes in hydrological extremes [58, 57, 82]. Numerous studies have investigated the impact of weather and climate on corn, soybean and wheat crop yields in the U.S. Midwest and GLB [9, 15, 43, 62, 77, 91]. Within the GLB, the southern states (i.e., Michigan, Illinois, and Indiana) are projected to experience the most substantial negative effects, with maize particularly vulnerable to drought stress [100]. Despite potential declines in productivity, agriculture is anticipated to persist as a crucial land use in the GLB, thanks to adaptation strategies such as irrigation, new crop varieties, and altered management practices [3, 37]. However, as climate change continues to exacerbate the unpredictability of extreme hydrological events, continuous efforts in revising the adaptation strategies to best fit these conditions are crucial. Thus, understanding the impacts of climate change on the timing and magnitude of the hydrologic cycle in the GLB will help inform the mitigation and adaptation strategies to implement for a sustainable future.

1.1.2 Infrastructure

Climate change will also have adverse impacts on infrastructure, including dams, across the GLB [60]. Currently, there are thousands of dams in the GLB. Fluctuation in river discharge, as exasperated under climate change, could cause increase the potential for devastating failures. On average, dams in the GLB are over 80 years old. Up to 78-97% of these dams are classified as high hazard potential according to the USACE, meaning they could cause adverse consequences, including significant loss of water for human uses, economic losses, environmental damage or deaths in the event of failure or mis-operation (USACE National Inventory of Dams, [65, 60]). Thus, it is imperative that we understand how and why streamflow changes over time in order to properly assess dam risk. Figure 1.3a shows dams in the GLB, colored by their primary purpose, as listed on each state's Department of Environmental Quality (DEQ) website. Figure 1.3b shows

a histogram of the year in which the dams were built.

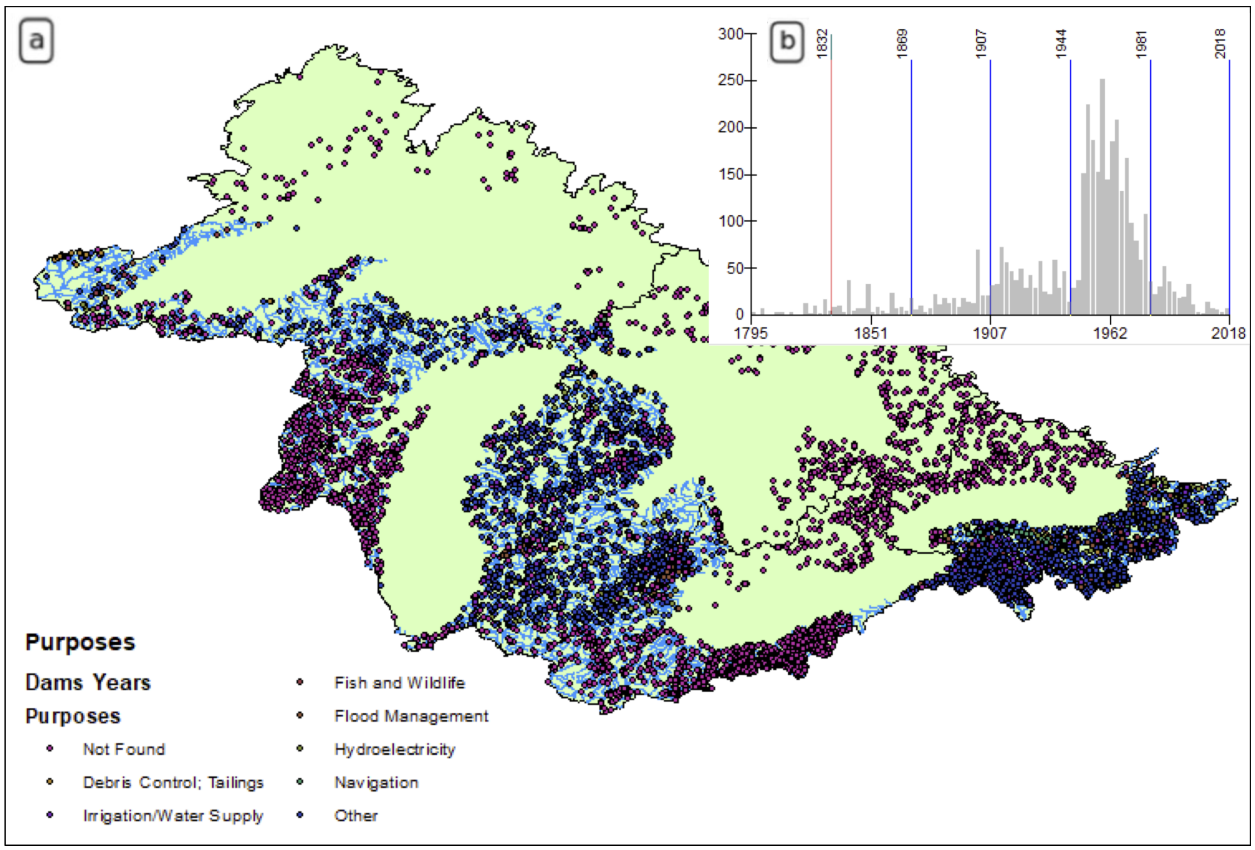

Figure 1.3 Dams in the Great Lakes Basin.

1.2 Research Motivation

Previous studies point to significant changes in timing and magnitude of hydrological events throughout the region by the end of the 21st century but lack a comprehensive and detailed analysis on the impacts of climate change on water availability in the GLB. It is projected that climate change will bring more intense rainfall events and higher temperatures summer, leading to an increase in frequency and magnitude of intense storms and floods, and heatwaves and drought events [10, 16, 17, 20, 26, 80]. Many of these previous studies have focused on historical trends [27, 44, 66], sub-basins of the GLB [21] or limited future projections using downscaled climate data [17]. Older studies examine climate change impacts under older and different climate change conditions [69]. Thus, to fill the gaps, here, I provide a comprehensive spatial and temporal analysis

of changes in hydrodynamic variables and analysis of different climate change scenarios building on previous works to provide better understanding of potential spatial and climate-driven changes in the GLB.

1.2.1 Agriculture

The changes in climate, especially changes in rainfall and runoff patterns, could be particularly challenging for agriculture as it is especially vulnerable to extreme hydrological events [72], which can lead to soil erosion, waterlogging, heat stress, and, ultimately, decreased crop yields [47, 72, 91, 93].

1.2.2 Infrastructure

Infrastructure such as dams will also face hardship in the face of climate change [60]. Because the dams in the region are small, they are understudied. Although hydropower production is not the primary purpose of most dams in the region, hydropower dams do produce a significant portion of energy throughout various states, making them critical infrastructure in the 21st century [29, 52, 81] . The impacts of climate change on this critical infrastructure in the GLB has not been investigated.

1.3 Research Goals, Objectives, and Scientific Questions

1.3.1 Objectives

- **Objective 1: Impacts on Water Quantity:** Firstly, I will examine the impacts of climate change on water quantity in the region.
- **Objective 2: Impacts on Food:** Next, I will assess the impacts of climate change and extreme weather events on food production and availability in the region by examining changes in hydrology during critical agricultural seasons throughout the basin's agricultural areas.
- **Objective 3: Impacts on Infrastructure:** Lastly, I will assess impact of extreme weather events (floods and droughts) on dam infrastructure by examining the changes in high flows throughout the 21st and at dams locations.

1.3.2 Questions

The key science questions in this study are:

1. What are the projected changes in hydrodynamics and extreme hydrological events in the Great Lakes region under different climate scenarios?

2. How will these changes affect different sectors and communities in the region, and what are the most effective adaptation and mitigation strategies to manage water resources?

1.4 Thesis Outline

This thesis has 5 chapters, including the introduction. Given the rationale and purpose of the thesis, the chapters are designed to contribute to address the objectives stated above. Chapter 2 gives a detailed description of the methods and data utilized in the study. Chapter 3 details the results of a preliminary analysis of historical data and analysis on infrastructure in the GLB. Chapter 4 assesses several potential impacts of climate change on the hydrology within the GLB. Chapters 5 and 6 assess the societal implications of climate change on agriculture and dam infrastructure, respectively. Finally, concluding remarks are presented in Chapter 7.

CHAPTER 2

DATA AND METHODS

The Catchment-based Macro-scale Floodplain model (CaMa-Flood) [98] was employed to simulate streamflow under various climate scenarios. The model was first validated using reanalyzed hybrid historical runoff data from ISIMIP3a (Inter-Sectoral Impact Model Intercomparison Project Phase 3) and compared with observed data from stream gauge stations across the GLB [96, 94]. Then, reanalyzed hybrid forcing data from ISIMIP3b were used to build an ensemble of projected future conditions under three carbon emissions scenarios through the 21st century, RCP 2.6-SSP1, RCP 4.5-SSP3 and RCP 8.5-SSP5 [96, 95]. Hydrodynamic data such as streamflow, river depth, flood depth, water surface elevation and surface water storge were analyzed through the lens of water availability for agriculture and the results are presented in this study.

2.1 Data

2.1.1 Observed Data

Observed river discharge was obtained from gauging stations throughout the GLB for historical analysis and model validation. This data was collected from USGS WaterWatch current and historical streamflow observations (U.S. Geological Survey, 2016). To validate the model performance, daily observed discharge data between 1989-2013 was obtained from 11 USGS gauging stations across the GLB. The following gauging station selection criterion were employed:

- Continuous data from the validation period (1989-2013)
- Larger rivers: more than 30 cubic meters per second average discharge
- Wide rivers: more than 90 m wide.

Figure 2.1 below details the station number, as shown in further figures in this study, station ID and name and drainage area in square miles (mi^2).

Table 2.1 Selected USGS gauging stations.

Station	Station ID	Station Name	Drainage Area (mi^2)
1	4024000	St. Louis River at Scanlon, MN.	3,430
2	4067500	Menominee River near McAllister, WI	3,920
3	4082400	Fox River at Oshkosh, WI	5,310
4	4101500	St. Joseph River at Niles, MI	3,666
5	4119000	Grand River at Grand Rapids, MI	4,900
6	4122001	Muskegon River at Bridge Street at Newaygo, MI	2,400
7	4157005	Saginaw River at Holland Avenue at Saginaw, MI	6,060
8	4193500	Maumee River at Waterville, OH	6,330
9	4231600	Genesee River at Ford Street Bridge, Rochester, NY	2,474
10	4249000	Oswego River at Lock 7, Oswego, NY	5,100
11	4260500	Black River at Watertown, NY	1,864

2.1.2 Model Input Data

Gridded runoff data for simulation was obtained from ISIMIP [96]. In ISIMIP, impact modelers utilize climate model simulations, known as global climate model (GCM) outputs, as inputs to sector-specific impact models. These GCM outputs serve as inputs to capture future climate conditions, encompassing variables like temperature, precipitation, and other pertinent factors. To enhance the accuracy of the impact models, climate inputs are integrated with additional data sources, including land use, socio-economic indicators, and greenhouse gas emissions scenarios. Through simulations, these models estimate the potential consequences of the climate conditions on respective sectors, generating output data that enables inter-model comparison and evaluation. Data for ISIMIP is obtained from diverse sources, encompassing international climate model intercomparison projects and global climate model archives. ISIMIP data had been bias corrected pre-use with various additional data sources and are designed to adjust for changes in land cover, socio-economic indicators, and greenhouse gas emissions to enhance simulation accuracy [56]. The runoff datasets were generated on a 0.5°x0.5° latitude-longitude grid.

A total of 15 model combinations were utilized, with 15 historical simulations and 45 future projections. The ensemble mean of all the model combinations used was calculated and used for analysis. 2.2 provides a detailed list of the hydrological and climate models used in this study. Note

that SSP refers to Shared Socioeconomic Pathways, and RCP refers to Representative Concentration Pathways.

2.1.2.1 Historical Runoff

For model validation, input runoff data for the hydrodynamics model was obtained from ISIMIP3a [94]. For a calibration and validation period of 43 years (1971-2014), total runoff, qtot (kg m-2 s-2), was generated from hydrological models CWatM, H08 and WaterGAP2-2e, each forced with global meteorological forcing data processed from 6 climate models, one using observed atmospheric climate data from the Global Soil Wetness Project (GSWP-W5E5) for uncertainty analysis in variation in the other climate models. The climate models selected were GFDL-ESM4 (Geophysical Fluid Dynamics Laboratory Earth System Model version 4.0), IPSL-CM6A-LR (Institut Pierre-Simon Laplace Low Resolution Climate Model version 6.0), MPI, MRI and UKESM1.

2.1.2.2 Future Projected Runoff

For future projections, input runoff data for the model was obtained from ISIMIP3b [95]. Datasets were obtained from hydrological models CWatM and H08, each forced with atmospheric data from earth system models GFDL-ESM4 (Geophysical Fluid Dynamics Laboratory Earth System Model version 4.0), IPSL-CM6A-LR (Institut Pierre-Simon Laplace Low Resolution Climate Model version 6.0) MPI, MRI and UKESM1, each for 3 emissions scenarios: SSP126, SSP370 and SSP585 as well as an additional 43-yearlong historical period (1971-2014) to provide the model with sufficient spin-up and to examine uncertainties caused by the input atmospheric forcing data.

Table 2.2 Input runoff data from hydrological and climate models.

Hydrological Model	Climate Model	Scenarios
CWatM	GFDL-ESM4	SSP1-RCP2.6, SSP3-RCP7.0, SSP5-RCP8.5
	IPSL-CM6A-LR	SSP1-RCP2.6, SSP3-RCP7.0, SSP5-RCP8.5
	MPI-ESM1-2-HR	SSP1-RCP2.6, SSP3-RCP7.0, SSP5-RCP8.5
	MRI-ESM2-0	SSP1-RCP2.6, SSP3-RCP7.0, SSP5-RCP8.5
	UKESM1-0-LL	SSP1-RCP2.6, SSP3-RCP7.0, SSP5-RCP8.5
H08	GFDL-ESM4	SSP1-RCP2.6, SSP3-RCP7.0, SSP5-RCP8.5
	IPSL-CM6A-LR	SSP1-RCP2.6, SSP3-RCP7.0, SSP5-RCP8.5
	MPI-ESM1-2-HR	SSP1-RCP2.6, SSP3-RCP7.0, SSP5-RCP8.5
	MRI-ESM2-0	SSP1-RCP2.6, SSP3-RCP7.0, SSP5-RCP8.5
	UKESM1-0-LL	SSP1-RCP2.6, SSP3-RCP7.0, SSP5-RCP8.5
WaterGAP2	GFDL-ESM4	SSP1-RCP2.6, SSP3-RCP7.0, SSP5-RCP8.5
	IPSL-CM6A-LR	SSP1-RCP2.6, SSP3-RCP7.0, SSP5-RCP8.5
	MPI-ESM1-2-HR	SSP1-RCP2.6, SSP3-RCP7.0, SSP5-RCP8.5
	MRI-ESM2-0	SSP1-RCP2.6, SSP3-RCP7.0, SSP5-RCP8.5
	UKESM1-0-LL	SSP1-RCP2.6, SSP3-RCP7.0, SSP5-RCP8.5

2.2 Model

CaMa-Flood is a high-resolution hydrodynamics model that simulates river discharge, water storage and flood inundation dynamics on a large scale. The model utilizes a high resolution (3-minute) global topography map, as well as a sub-grid flow direction map (MERIT-Hydro). The model is driven by runoff data generated by hydrological or land surface models. The model then simulates hydrodynamic conditions, including discharge, water level and flood depth, across the specified region. Flood depth can be further downscaled to a resolution as low as 90 m.

In the CaMa-Flood model, a river network map is first generated within the specified region, which describes the upstream-downstream relationship of river sub-catchments among and within cells. Then, the model utilizes the inertial wave equation, which is part of the St. Venant conservation of momentum equation (below) to calculate discharge in each cell.

$$\frac{\partial Q}{\partial t} + \frac{\partial}{\partial x}\frac{(Q^2)}{A} + \frac{gA\partial(h+z)}{\partial x} + \frac{gn^2Q^2}{R^{\frac{4}{3}}A} = 0 \tag{2.1}$$

where:

Q : discharge

A : flow cross-section area

h : flow depth

z : bed elevation

R : hydraulic radius

n : Manning coefficient

g : acceleration due to gravity

h : friction slope

Next, total water level and inundated area are then calculated, based on the conservation of mass (below) [98].

$$S_i^{t+\Delta t} = S_i^t + \sum_k^{Upstream} Q_k^t \Delta t - Q_i^t \Delta t + A c_i R_i^t \Delta t \tag{2.2}$$

where:

S_{t+1} : cell storage

Δt : time step

Q_{t_k} : cell inflow

Q_{t_i} : cell outflow

A_{c_i} : cell area

R_{t_i} : cell input runoff

In this study, CaMa-Flood was regionalized to an area 15 degrees latitude (37.5N to 52.5N) by 30 degrees longitude (65W to 95W) and simulated at a resolution of 3 arc-minutes (5 km at the equator) over a historical period of 43 years (1971-2014) using 15 hydrological and climate model combinations. The historical simulation was then used as initial conditions for future simulation

of the next 85 years (2015-2100) under the 3 Socioeconomic Development Pathways (SSP). For analysis, the future projection period was split into 25-year periods: Early-Century (2025 – 2050), Midcentury (2051-2075) and Late-Century (2075-2100).

2.3 Statistical Analysis

Various statistical metrics were applied to evaluate model performance including a ratio of mean annual water volume (bias), ratio of the standard deviation of annual water volume (standard deviation), correlation coefficient (R), and the Kling-Gupta Efficiency (KGE) [36] . Flood risk and storm return periods, as well as drought return periods were calculated using [13]. Drought risk parameters such as magnitude and occurrence were calculated using a simple streamflow index [70]. Finally, historical return periods of high and low flows were calculated, assessing the longevity and magnitude of droughts, and compared with projected data provide insights into the timing and magnitude of changing seasonal droughts, rainfall, and streamflow patterns influenced by climate change.

2.3.1 Flood Return Periods

Flood return periods were calculated using methods analogous to [13]. The Peak over Threshold (POT) method was utilized to determine a frequency curve to examine changes in the frequency and magnitude of extreme floods and droughts in future periods [12]. Return periods of 10, 25 and 50 years were included in the analysis. Equation 1 shown below describes the magnitude, x, of a flood event with a return period of T years. Equation 2.3 describes POT.

$$x = B \ln\left(\frac{T}{T_0}\right) + x_0 \tag{2.3}$$

where:

x : discharge magnitude

T : return period of discharge with magnitude x

x_0 : base or selected minimum value of x

T_0 : return period of discharge with magnitude x_0

B : the slope parameter of distribution (the population standard deviation)

2.3.2 Drought Analysis

Hydrological drought in the GLB was assessed using the Streamflow Drought Index (SDI) [70]. The SDI is a simple way to characterize the severity of hydrological drought, using an approach analogous to the Standardized Precipitation Index (SPI) for meteorological drought. The SDI is calculated as the standardized cumulative streamflow volume for overlapping 3-, 6-, 9- and 12-month periods within each hydrological year. SDI values below zero indicate drought conditions which are classified into categories of mild, moderate, severe and extreme drought based on set thresholds [70]. In this study, drought magnitude was calculated using the SDI and drought occurrence was counted each day whether SDI was <0. The SDI is defined by equation 2 below. Drought state, severity and criterion are described in the table below.

$$SDI = \frac{x_i - \bar{x}}{s} \tag{2.4}$$

where:

x_i : daily discharge

$\bar{x}$: historical mean of the discharge calculated from the entire historical period

s : tandard deviation of discharge calculated from the entire historical period

Table 2.3 presents the classification of drought severity based on the SDI. The SDI values determine the level of drought severity, with different states ranging from non-drought conditions to extreme drought conditions. The criterion column specifies the SDI thresholds corresponding to each drought state.

Table 2.3 Drought severity classification based on Streamflow Drought Index (SDI).

State	Description	Criterion
0	Non-drought	$\text{SDI} \geq 0.0$
1	Mild drought	$-1.0 \leq \text{SDI} < 0.0$
2	Moderate drought	$-1.5 \leq \text{SDI} < -1.0$
3	Severe drought	$-2.0 \leq \text{SDI} < -1.5$
4	Extreme drought	$\text{SDI} \leq -2.0$

2.4 Model Validation

Validation of the seasonal cycle of simulated river discharge is presented in figure 2.1. The agreement between observed and the ensemble mean of simulated river discharge values was generally agreeable with the mean volume bias of 1.05, meaning there's only a 5% over- or underestimation of the simulated discharge compared to observed. The model captured flows with high accuracy as most of the simulations flow predictions were within 1 standard deviation of the observed streamflow. Furthermore, the timing of the model was also good, with the correlation of all stations being between 0.78 and 0.94. The KGE varied greatly from station to station but was also generally good, with the maximum being 0.92 and the minimum positive value being 0.2. A more detailed view of the agreement between the observations and individual model simulations may be obtained from the Taylor Diagram [87].

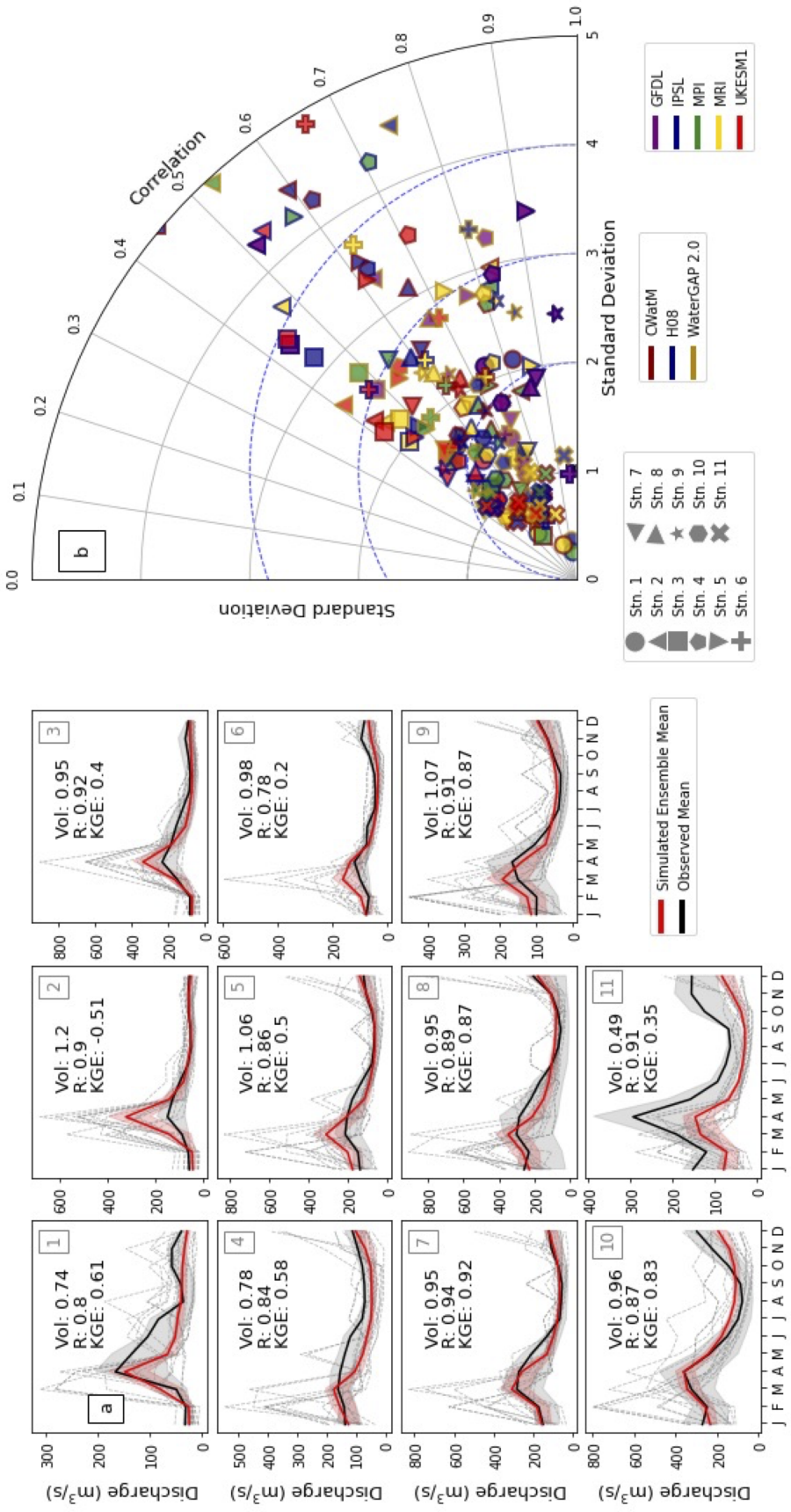

Figure 2.1 Hydrographs and Taylor Diagram for model validation.

Figure 2.1 shows the tong-term (1989-2013) comparison of simulated and observed river discharge (a1-11) at the selected USGS gauging stations. Shadings (red for the ensemble of river discharge simulations and grey for the observations) indicate interannual variability presented as the first standard deviation above and below the mean for each month. Volume bias (Vol), correlation coefficient (R) and Kling-Gupta efficiency (KGE) are indicated for each station in the upper right corner of each panel. Panel b shows a Taylor Diagram [87]; the symbol shape represents the gauging station, the edge color of the shape represents the climate model used in the simulations and the fill color represents the hydrological model used in the simulations.

A detailed view of the agreement between the observations and individual model simulations may be obtained from the Taylor Diagram [87] presented in Figure 2.1b, which show, for each data set at each gauging station, the correlation and the standard deviation compared to the observed data. In general, CWatM hydrological model and MRI climate model each had the best overall performance, and the H08 hydrological model performed the worst, but these results vary with each individual gauging station. Conversely, the H08 hydro model paired with the UKEMS climate model appears to have the least favorable performance.

Validation of simulated long-term average seasonal cycle of river discharge (red lines) to observation from USGS (black lines) at selected locations shown in Figure 2.2. The color-coded shadings indicate interannual variability presented as the first standard deviation above and below the mean of each month. Volume bias (Vol), correlation coefficient (R) and Kling-Gupta efficiency (KGE) are indicated for each station in the upper right corner of each panel.

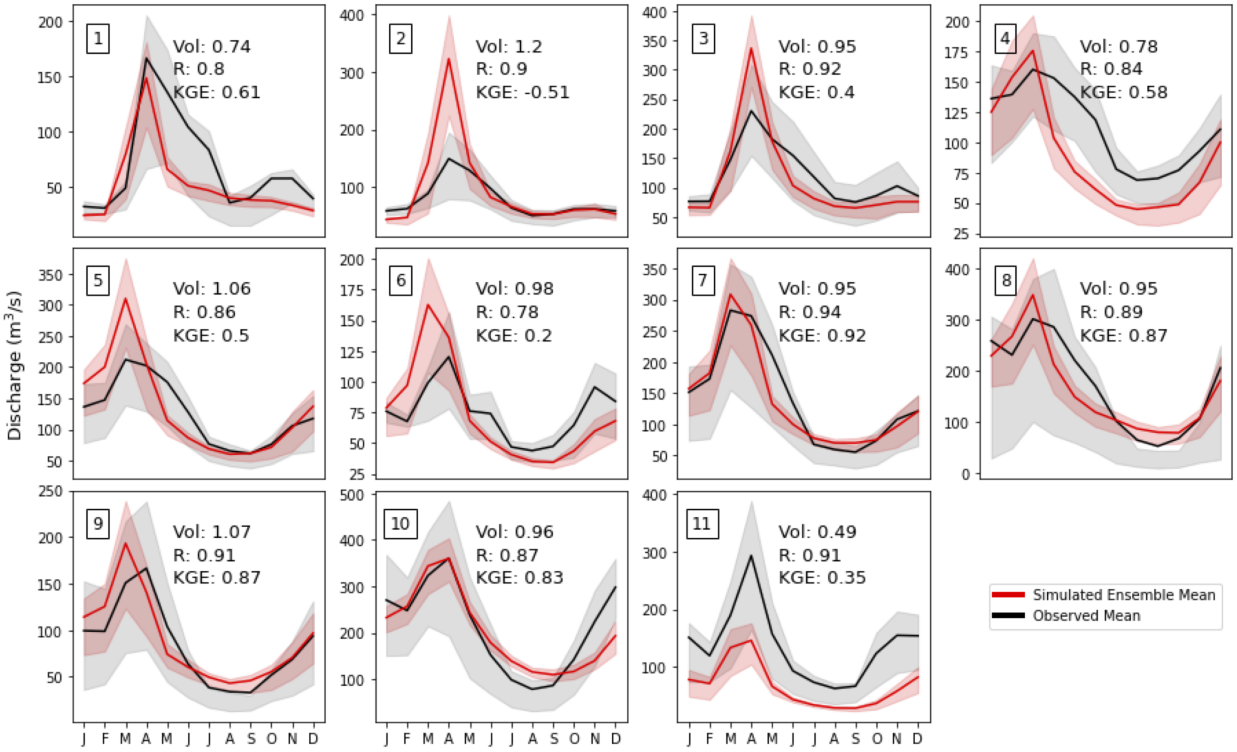

Figure 2.2 Hydrographs for the validation of the ensemble mean.

Some model-observation discrepancies could be attributed to many factors including uncertainties in forcing data, model parameters (e.g., channel width, Manning's coefficient) and physical attributes (e.g., dams, land use, proximity to the Great Lakes). Model performance was best at the stations in the middle of the basin, rather than closer to the Great Lakes – close proximity to the lakes caused routing issues in the model. Given the complexity of river-floodplain hydrodynamics and the use of a large and basin-wide model, I consider these results to be reasonable, especially to assess the effects of climate change on the hydrodynamics of the GLB. Overall, the accurate simulation of discharge at the 11 stations provides confidence that the model reasonably simulates various hydrodynamic attributes around the GLB.

CHAPTER 3

CLIMATE CHANGE AND DAM INFRASTRUCTURE

Climate change will also have adverse impacts on infrastructure, including dams, across the GLB [60]. Increasingly high volumes of river discharge anticipated under climate change could increase the potential for devastating failures. On average, dams in the GLB are over 80 years old [29]. A high proportion are classified as high hazard potential according to the USACE, meaning they could cause significant loss of water for human uses, economic losses, environmental damage or deaths in the event of failure or mis-operation (USACE National Inventory of Dams) [65]. Thus, is imperative to understand how and why streamflow changes over time in order to properly assess dam risk.

Overall, it is important to understand the relationship between climate change, dam infrastructure and streamflow in the GLB to allow for better planning in water resources management. Thus, in this study, I address questions on whether streamflow has changed, how it has changed and investigate the main factor driving the changes: climate change or dam operations.

3.1 Dam Information

Dam information, including name and location, primary purpose, river name, year built, and storage capacity was collected from the US Army Corps of Engineers' National Dam Inventory Website. A total of 2,276 dams were analyzed there throughout the GLB. A complete list of dams for each state surrounding the Great Lakes was downloaded, merged and sorted to include only the ones within the GLB boundary (Figure 3.1). Dams are depicted based on their size and age. Gauging stations with 25 years or more data are depicted as black circles.

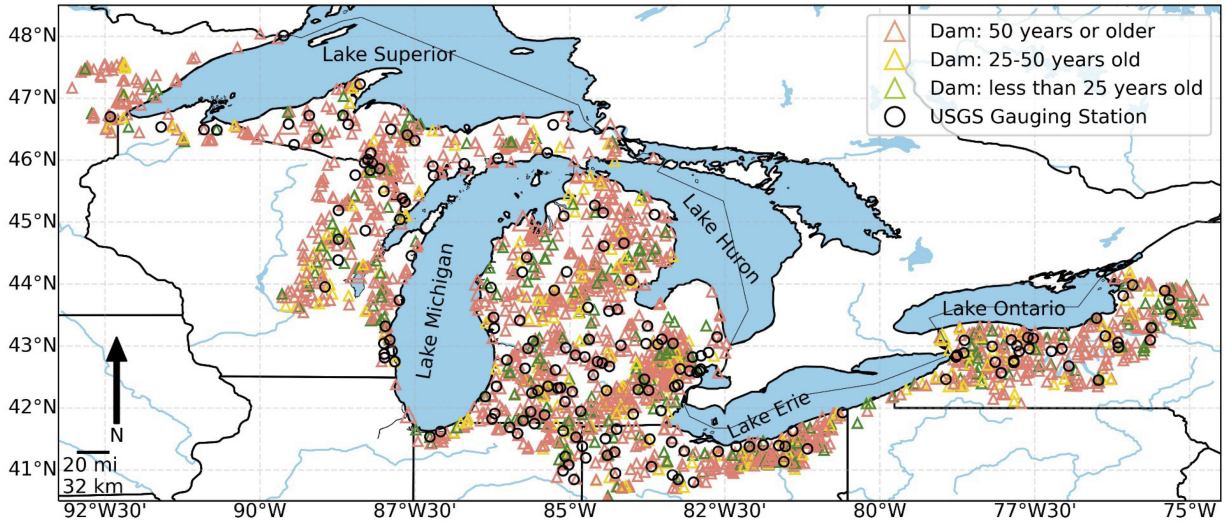

Figure 3.1 Map of the GLB dams and USGS gauging stations.

3.1.1 Statistical Analysis

The first aim of this study was to analyze spatial and temporal trends in streamflow. Firstly, the non-parametric Pettitt test was used for analyzing data homogeneity and determining major change-points within the datasets, next the Mann-Kendall test and Sen's slope estimator were used for trend analysis, and finally, then Pruned Exact Linear Time (PELT) method was used to detect multiple temporal change-points in the time series.

The Pettitt test is a statistical tool used to determine whether a dataset is homogenous throughout [76] and pinpoint a location where there is a significant change in the dataset trend. The Pettitt test is especially useful in analyzing natural datasets because there are no underlying assumptions that the data must be distributed normally, thus this test is not deterred by outliers or skews in distribution [74].

Next, the Mann-Kendall test was used to investigate monotonic changes in monthly and annual streamflow. Monotonic trends are consistent increases or decreases through time that may not be linear [4]. This test can be used in place of a traditional linear regression analysis to determine whether the slope of a regression line in a dataset is zero [8]. Later, Kendall's rank correlation coefficient, τ, was integrated to measure the association between points in the dataset [49], increasing

the accuracy of results [4]. Along with the Mann-Kendall test, Sen Slope estimator was used to determine the magnitude of the change in a dataset [76]. Rather than using a traditional method of linear regression, Sen Slope does not require that data be normally distributed. Sen Slope estimator is widely used to examine monotonic trends in a dataset, as well as any hidden sub-trends [4]. This method does not need to account for cyclical patterns, i.e. seasonal cycles, or the length of the dataset, or missing data points [4, 5, 76].

Lastly, change point detection (PELT method) was used to identify multiple points in the dataset where trends emerge [75, 76]. In large datasets, there may be multiple points of changes in trends [90]. The change points are calculated using a basic change point detection equation, a penalty factor, and a data pruning window. This method identifies minimum values within windows of the dataset, and then analyzed surrounding windows to determine whether it is the true location of the point [51].

3.2 Results

3.2.1 Streamflow Variation

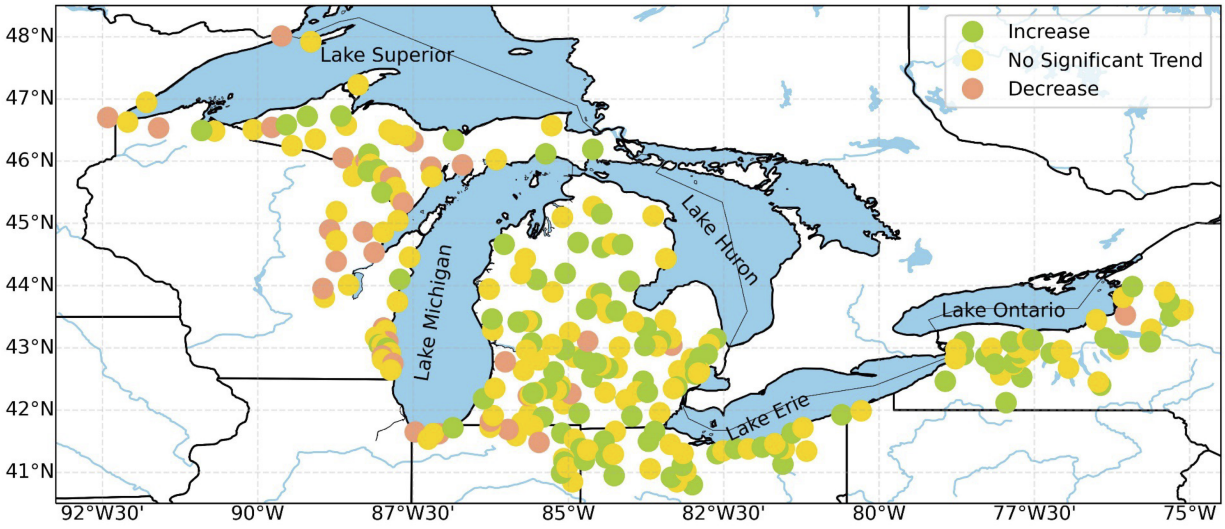

Figure 3.2 Map of USGS streamflow trend of data over time.

Based on the results of the Mann-Kendall test and Sen's Slope Estimator, a map of the USGS stations with 25 of more years of data was created, the location of each station was plotted based

on trend (Sen's Slope coefficient): whether it showed an increasing (green), decreasing (pink) or no significant trend (yellow).

Overall, it appears that streamflow has increased throughout the region. According to our analysis, streamflow has increased more throughout the Eastern parts of the region, and it has decreased more throughout the Western parts of the region. Approximately 86% of the stations showing a decreasing trend were located west center of the basin latitude line(85° W), while only 3 stations were located east of this line. Additionally, more than half of the streamflow gauges in the east showed increasing trends, whereas in the west, only about a third showed increasing trends. There appears to be fewer dams in the western part of the basin, this may have had an impact on the streamflow throughout this region.

3.2.1.1 Dam Impacts on Streamflow

I examined 18 gauging stations that were immediately downstream from and built at least 5 years after dams. Figure 3.3 shows the seasonal discharge at the following stations (a) Menominee River at US Hwy 2 near Iron Mountain, MI; (b) Huron River at Ann Arbor, MI; (c) Milwaukee River at Milwaukee, WI; and (d) Black River at Watertown, NY. Through visual analysis of monthly average streamflow hydrographs before and after the dam was built, our analysis revealed that the dams have impacts on the seasonal flow. For instance, as seen in the figures below (Figure 3.3), the dams commonly increase low-flow during dry seasons and decrease high-flow during wet seasons (Figure 3.3 a, b, d). This can help mitigate damage from floods and meet water demands during droughts. Additionally, these dams often release more water as the wet season is ending, likely to support agriculture (Figure 3.3 a, d). Furthermore, the dams also may release more water in the driest and coldest months of the year, preparing for melting seasons which may otherwise cause flooding (Figure 3.3 b, c). The impact of the dams on overall water balance was negligible, as the total amount of yearly discharge before and after the dam was built was the same. However, if the total amount of yearly discharge increased or decreased significantly after the dam was built, then there must have been significant upstream changes to the river such as rerouting, reservoirs, or other dams. This was rare, as all the dams in this region are relatively small. Lastly, the impact

of dams, as seen in all the figures (Figure 3.3 a, is reduction in streamflow variation. I calculated the monthly average and standard error of monthly average streamflow and plotted them, as below (Figure 3.3).

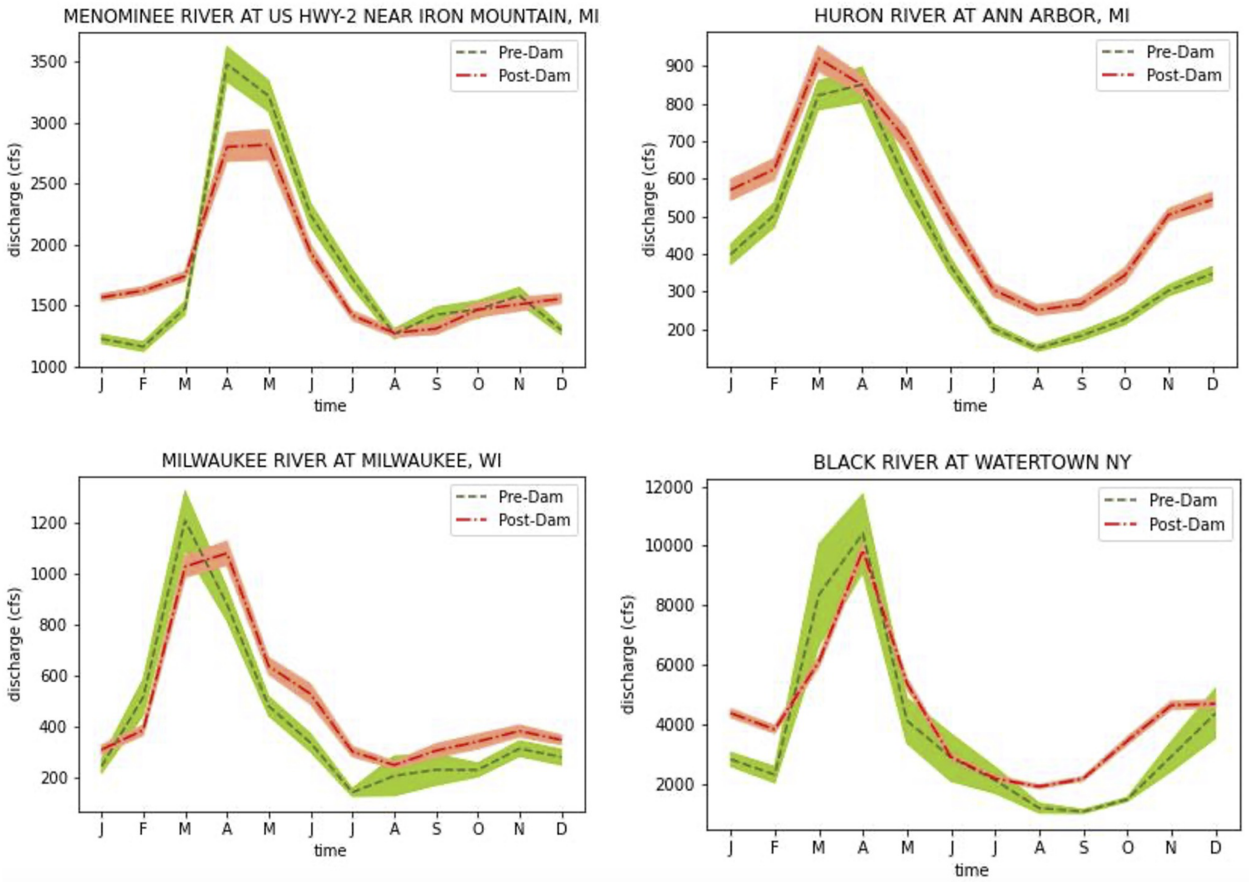

Figure 3.3 Seasonal historical discharge at selected stations.

To determine the impact of dams on streamflow, I performed change-point detection and the Pettitt test to find the location of significant change-points, then the Mann-Kendall Test and Sen's Slope Estimator to determine the direction and magnitude of the trend in streamflow. All the datasets showed a significant number of changepoints using the PELT method of change-point detection. At the 5% significance level, 17 of the 18 stations showed a statistically significant change-point, according to the Pettitt Test. Of the 17, 16 showed an increasing trend. The largest percent increase in average monthly streamflow after the change-point was 72.5%, while the largest

percent decrease was 10.4%. Results indicated that the change-point at most of the stations occurred between 1965 and 1980 (95% confidence interval) with a standard deviation of 14.5 years. As for the Mann-Kendall test, of the 18 stations, 13 were determined to show a statistically significant increasing trend, and none were decreasing. Results of the Sen's Slope estimator are as follows: the largest slope was 1.065 cfs/year. The smallest was 0.0047, however, this may have been a false positive, as this slope is quite slight compared to the others, including ones that resulted in no trends detected. The average change was an increase of 0.1475 cfs/year, with a standard deviation of 0.2436 cfs/year. The only station that showed no trend according to the Pettitt Test also showed no trend according to the Mann-Kendall Test. However, there were 4 stations that showed a change point according to the Pettitt Test but no trend according to the Mann-Kendall test.

After performing changepoint detection, I compared this result to the year the dam was built. It was found that the dam construction year was generally before or after the largest change-point; therefore, the dam could not have impacted streamflow. For instance, in figure 3.4, data for one selected station (Manistique River near Manistique, MI) is plotted, along with the dam-year and the changepoint-year. The dam did not impact streamflow, as it was built 11 years before the changepoint was detected. All the datasets showed several changepoints using the PELT method. These were interpreted to be dry-periods and wet-periods. They are significant, as they show that these kinds of wet and dry patterns are cyclical and are not caused by climate change. It was a reoccurring pattern that drier periods occur more frequently and have longer duration later in the data than earlier.

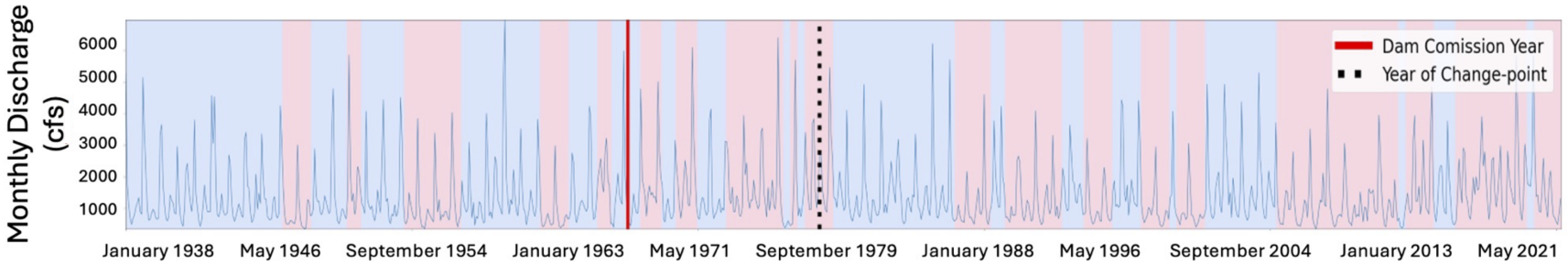

Figure 3.4 Time series of discharge at selected station, with change point detection.

After these tests were performed, the year the dam was built was compared to the year in which the change point was detected to determine the impact of dam construction and operation. The smallest difference in the change-point-year and the dam-year was 1.5 years, while the largest difference was 56.5 years. In total, 11 out of 17 change-points were detected after the dam was built (by at least 2.5 years), and the rest were detected before the dam was built.

3.2.1.2 Climate Change Impacts on Streamflow Magnitude

As for stations that were not downstream from dams, the Pettitt Test was performed on 254 stations, and of these, a statistically significant change in mean monthly average streamflow was detected at 233 of them at the 5% significance level. Results indicated that the change-point in most rivers (95% confidence interval) occurred between 1987 and 1991. The mean year was 1989 and the standard deviation was 17.3 years, which was very large while the sample was also quite large at 254 stations analyzed. The distribution of the year of change-point detection was roughly bimodal, with the largest number of change-points being in the 1980s, and the second largest number of change-points being in the 2010s. Further, the Mann-Kendall Test and Sen's Slope Estimator were performed on these 254 stations, 87.8% of which showed a statistically significant trend in streamflow: 66.5% increasing and 3.94% decreasing. Results of the Sens' Slope estimator are as follows: the largest increasing trend was 257.65 cfs/year, however this seemed to be an outlier, and the largest decreasing trend was -0.6398 cfs/year. The average slope before removing the high outlier is an increase of 1.236 cfs/year with a standard deviation of 16.23 cfs/year, and after removing the outlier, the average slope is an increase of .215 cfs/year with a standard deviation of .856 cfs/year. The largest percent increase in average monthly streamflow after the change-point was 354% and the next largest was 91.6%, while the largest percent decrease was 41.9%. The average change was an increase of 26.4%. All the datasets showed a significant number of changepoints using the PELT method.

Results indicated that the change-point at most of the gauging stations immediately downstream from dams (95% confidence interval) occurred between 1966 and 1980. The mean year was 1973 and the standard deviation was 14.5 years, which was very large while the sample size was very

small. On average, the change-point was detected 12 years after the dam was built, meaning the dam likely had minimal impact on streamflow. On the other hand, results from gauging stations analyzed regardless of proximity to dams indicated that the change-point in most rivers (95% confidence interval) occurred between 1987 and 1991, much later than the stations located downstream from dams. The sample size of gauging stations without dams was 254 while the sample size of gauging stations with dams was only 18, so this causes a large discrepancy between the datasets. Additionally, because it was found that dams do not have a significant contribution to changes in streamflow, the gauging stations immediately downstream from dams were also analyzed as part of the 254 gauging stations.

3.2.1.3 Climate Change Impacts on Streamflow Timing

Figure 3.5a shows a histogram of the mean day of maximum discharge for year 1970 and year 2000 at one station, demonstrating how spring timing has shifted over the past 50 years. Figure 3.5b shows a time series of day of maximum discharge over the past 50 years with a trendline. Figure 3.5c shows annual maximum discharge over the past 50 years with trendline.

The above figure displays a histogram of the timing of spring discharge for the year 1979 and the year 2000. As shown in the figure, the day of maximum discharge, or date of peak flow occurrence, has shifted earlier in the year in many stations. The top right figure shows a line graph with a trendline of the data. Consistent with the histogram, peak flow timing is shown to decrease throughout the years.

3.3 Discussion

Overall, due to a significant difference between the year of dam commission and the that a change-point was detected in the mean discharge, I found that dams have not significantly impacted downstream river discharge. Although dams did alter the timing and magnitude of seasonal flow, the overall amount of water traveling through the dams did not change significantly due to the activity of the dam.

Climate change, on the other hand, has been shown to cause changes in streamflow due to meteorological and hydrological changes. The effects of climate change have been reflected in

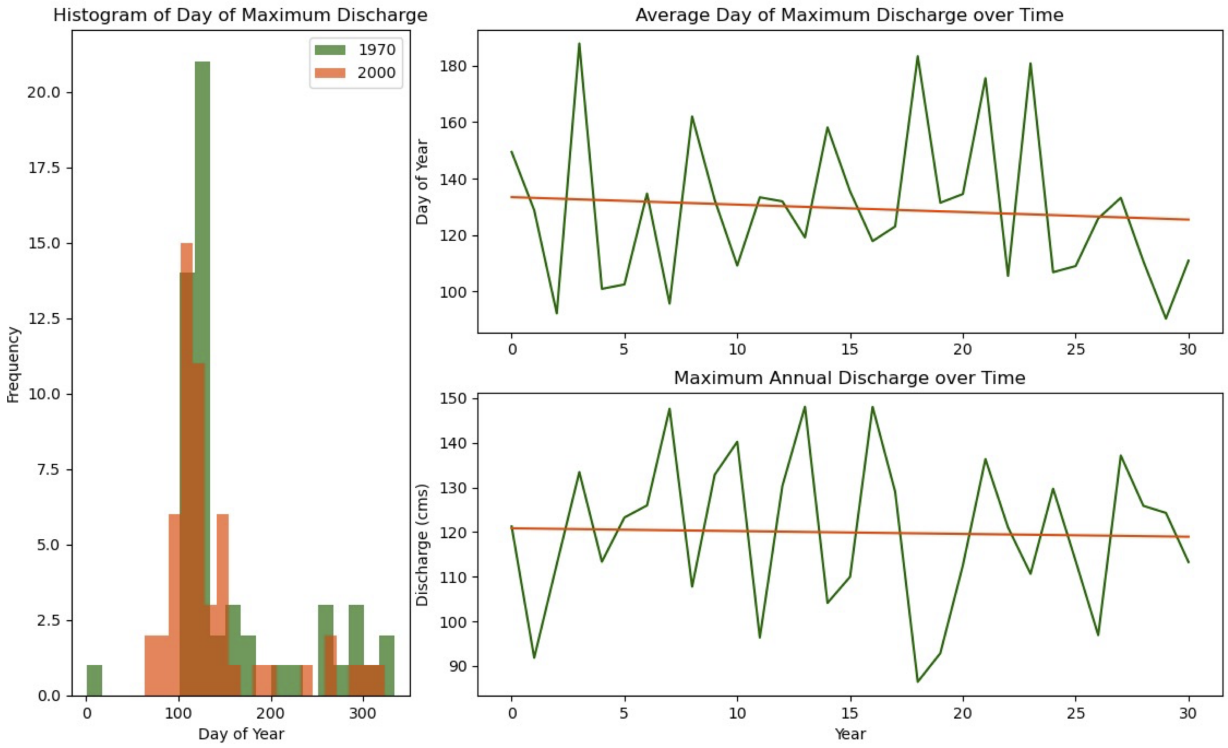

Figure 3.5 Historical change in maximum discharge timing.

the rivers of the Great Lakes region. Overall, the region has experienced more frequent and more intense hydrological extremes. For instance, rivers in the western portion of the region have seen a gradual decline in discharge volumes, whereas rivers in the eastern portion of the region have seen a gradual increase.

3.4 Conclusion

In this study, I examined historical observed streamflow data at USGS gauging stations to determine the impact of dams and climate change on streamflow. First, I found that dams have impacted the timing and magnitude of seasonal streamflow but have not significantly impacted the overall amount of discharge throughout the year. Dams in this region are primarily used for recreation or irrigation, therefore it is essential for them to be able to hold and release water, but not change streamflow significantly, as that would disrupt the natural balance of the environment. Additionally, I find that streamflow has increased at most of the gauging stations within the basin

throughout the recent decades. This increasing trend is more dominant throughout the eastern portion of the basin, but a decreasing trend is more dominant in the western portion of the basin. Second, I determine that these changes in streamflow are likely caused by climate change due to the low impact caused by dams, and the timing of the change being significantly before or after dam activity. The framework of this study can easily be applied to other works. The results of this study should be used to inform natural resource and water policy to prevent dam failure and mis-operation.

CHAPTER 4

PROJECTED CHANGES IN HYDROLOGY

Climate change has been shown to affect the water cycle, and, with this, higher temperatures have shown to be correlated with higher precipitation rates [42, 89]. Historically, precipitation has risen 14% since 1951 [89], and annual rates of evaporation have generally shown a slight increasing trend (CITE NOAA/USACE). Temperature affects precipitation. Temperature affects the dew point of air by increasing the vapor pressure deficit (VPD), allowing the atmosphere to hold more water [28, 89]. The higher the VPD, the more evaporation (E) and evapotranspiration (ET) occurs [78]. Once the atmosphere is saturated, water droplets condense, and precipitation begins [14, 89]. With increases in temperature, higher rates of E and ET cause more precipitation to occur because there is simply more water available in the atmosphere [97]. Figure 1.1b shows historical and projected daily average temperatures across the GLB. Temperature increases throughout the 21st century under all climate change scenarios are foretasted. These temperature changes induce changes in precipitation by allowing higher rates of E and ET. Overlake E is one of the dominating factors determining weather and climate in the GLB, as the lakes take up approximately a third of the total basin area. Figure 1.1c shows the historical and projected daily average precipitation rates across the basin. From these two figures, there is an evident, visual correlation between the two.

Such changes can influence overall water balance. Rises in annual total precipitation could lead to increases in the GLB's overall water balance (Huang2012). Surface water storage could consequently increase, as well as water levels in the Great Lakes. Increased temperatures and rates of precipitation could lead to increased river discharge, with significant alterations in peak flows and shifts in seasonal timing [16]. Lastly, floods could consequently become more frequent with this increase in water balance and higher occurrence of extreme hydrological and meteorological events under climate change [42].

These have important environmental, economic and societal implications, most critically on agricultural practices and infrastructure throughout the basin.

This chapter explores potential effects of climate change on the hydrology of the GLB throughout

the 21st century by investigating spatial and temporal changes in hydrodynamic conditions across the basin.

4.1 Streamflow

Changes in the seasonal streamflow regime reflect changes in annual conditions, including temperature and precipitation. This also can aid to predict local trends in projected conditions for extreme events like floods, droughts, and severe storms. These changes in seasonal streamflow suggest that there will be important changes in water resources management in the GLB in the coming decades [32, 89]. Seasonal flow regimes have important implications on water availability, specifically for agriculture and infrastructure including dams and irrigation.

Figure 4.1 compares the monthly means of historical and projected streamflow at each of the 11 selected USGS gauging stations. In figure 4.1, the black line depicts the historical period; future scenarios (SSP1, SSP3 and SSP5) are depicted in green, yellow, and red, respectively. The error bars show one standard deviation above and below the mean for each month under each scenario. Each hydrograph is annotated with the volume ratio (Vol) between the historical and given scenario from 2025-2100. The bar charts show the percent change in streamflow for each month for the future period as compared to the historical period under each climate change scenario.

Water balance, as calculated by the ratio of the projected annual average to the historical, increases in 9 out of 11 locations under all climate change scenarios by up to 10%. This is shown in Figure 4.1 with the volume ratio calculation and by visual comparison of the areas beneath the monthly streamflow curves. Additionally, our results agree with previous findings [40] that streamflow variation increases under each scenario in similar patterns where the largest changes (compare to historical) occur in the winter months and smallest in the summer months.

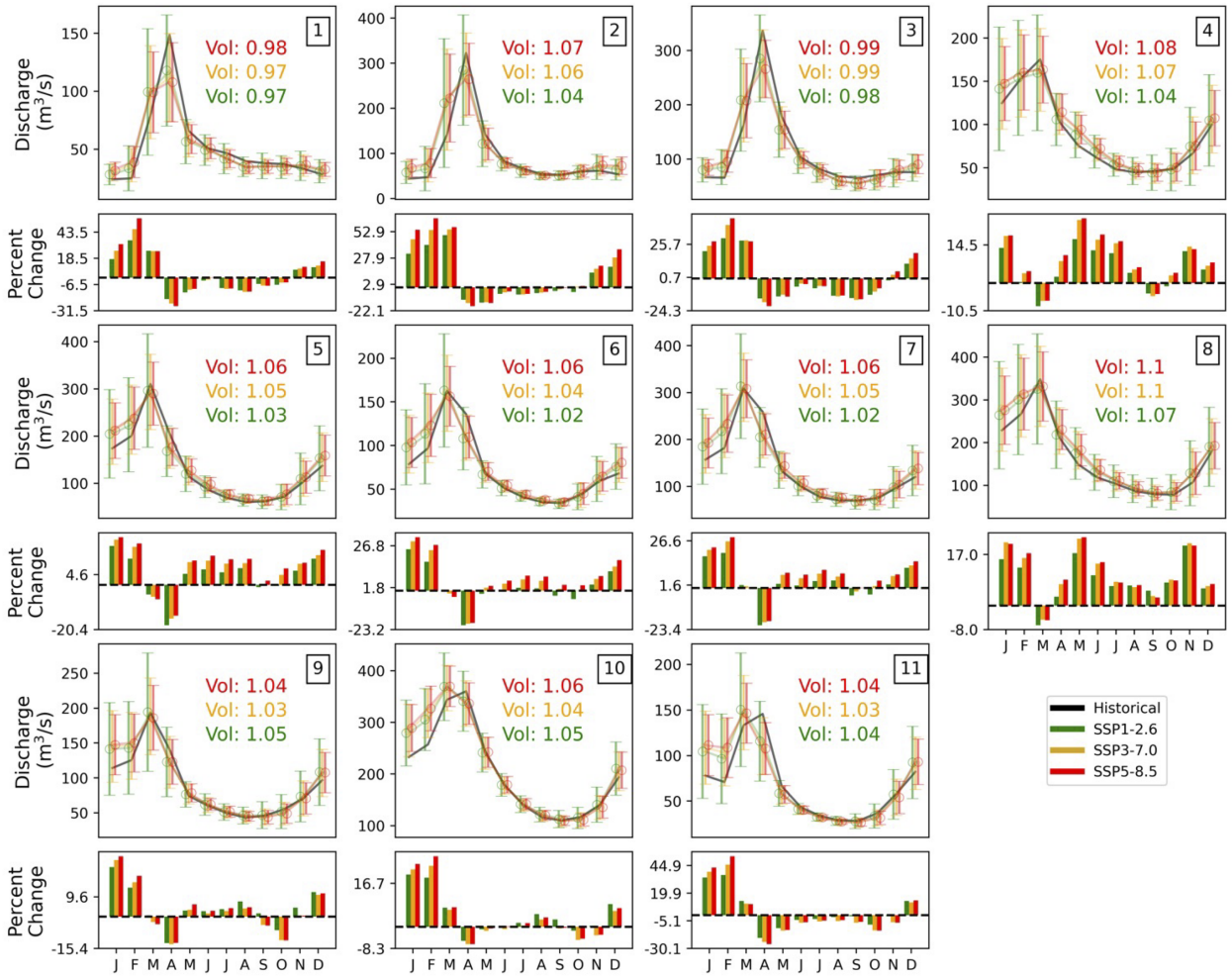

Figure 4.1 Projected annual mean seasonal discharge.

Next, Figure 4.1 depicts a substantial increase in winter discharge at each station from December to March, up to more than 50% at some stations. Notably, the most pronounced increase is observed under SSP5, while SSP1 exhibits the least. These results are in line with previous findings, which described similar changes in seasonal patterns in streamflow under scenarios SSP3 and SSP5 [16, 21, 23]. This increase is caused by an increase in winter runoff, caused by higher temperatures, higher rates of snowmelt and more precipitation as rainfall rather than snow. These results suggest an overall increase in the availability of water in the studied rivers, indicating more frequent and/or intense floods, pointing to the need for adaptation and mitigation strategies such as increased demand for water storage or diversion mechanisms [50, 92]. This could also contribute to higher

nutrient runoff and pollution [50].

Across all stations, a consistent decline in April peak flows by up to 40%. This decrease is consistent among scenarios. With relatively small increase in total water balance and a substantial increase in winter discharge, this suggests a shift in peak flow timing and potentially a shift in the start of spring [50]. This finding is consistent with previous findings, which suggested a shift in peak flow timing by up to a month, especially in northern, snowmelt dominated watersheds [16, 35].

As planting typically occurs in May and stations 4-8, which are located in agriculturally dominated areas project an increase of up to 20% in May discharge, there could be a risk of excess water, leading to waterlogged fields [47]. This "could make agricultural planting difficult and the potential for flooding more likely" [21]. This may cause adjustments in crop selection, planting schedules, fertilizer application, irrigation needs, and flood prevention strategies [50].

Interestingly, variation in seasonal streamflow was the smallest under SSP5 and largest under SSP1 consistently through all months at all stations. Variation decreased at 10 of 11 of the stations, suggesting more consistent rainfall patterns, however it is uncertain whether it is overall more or less. Variation decreased in summer months and increased during winter months at most stations. This increased variation in spring and summer discharge at some stations could make water availability less predictable, requiring adaptive flood prevention measures or irrigation adjustments [99].

Lastly, different regions (Western, Central, Eastern) show varied responses in summer streamflow. The Western Stations (Stations 1-3) experience a summer streamflow decrease of up to 10%, particularly in the later part of the season. Meanwhile, the Central Stations (Stations 4-8) show a significant increase in summer streamflow, ranging from 10-25% between May and September. However, the Eastern Stations (Stations 9-11) show no significant change in summer streamflow. These results align with results from regional studies such as [22], which suggest high variation in spatial patterns of streamflow due to different buffering capacities of different regions. The spatial and seasonal patterns in projected streamflow in the coming decades highlight the heterogeneity of climate change impacts on streamflow, emphasizing the need for region and season-specific including changes in agricultural practices (e.g. crop selection, planting dates, fertilizer utilization)

and irrigation demands [24].

Figure 4.1 compares the historical and projected seasonal river discharge patterns, examining the anticipated climate change-induced variations in seasonal streamflow and overall annual water balance. These projected changes in seasonal streamflow suggest that there will be important changes in water resources management for agriculture in the GLB in the coming decades.

4.2 Peak Flow Timing

Historically, in the GLB, peak river discharge has typically occurred in the springtime (March or April), when temperatures are increasing, causing snow on the ground to melt, and precipitation rates are high [33]. However, under climate change, since significant alterations in precipitation and temperature are anticipated, the timing of peak flows may also change [16, 73]. Anticipating shifts in peak flow timing is important because peak flows reflect water quality and water quantity at a certain point in time [30]. Changes in peak flow timing could induce cause changes in decision making for water resource allocation, most critically in infrastructure and agricultural management.

Figure 4.2 shows changes in peak flow timing under each scenario throughout the 21st century, with each scenario and period depicted in each panel (a-i), respectively. A red shade represents an earlier peak discharge date, while a blue shade represents a later peak discharge date.

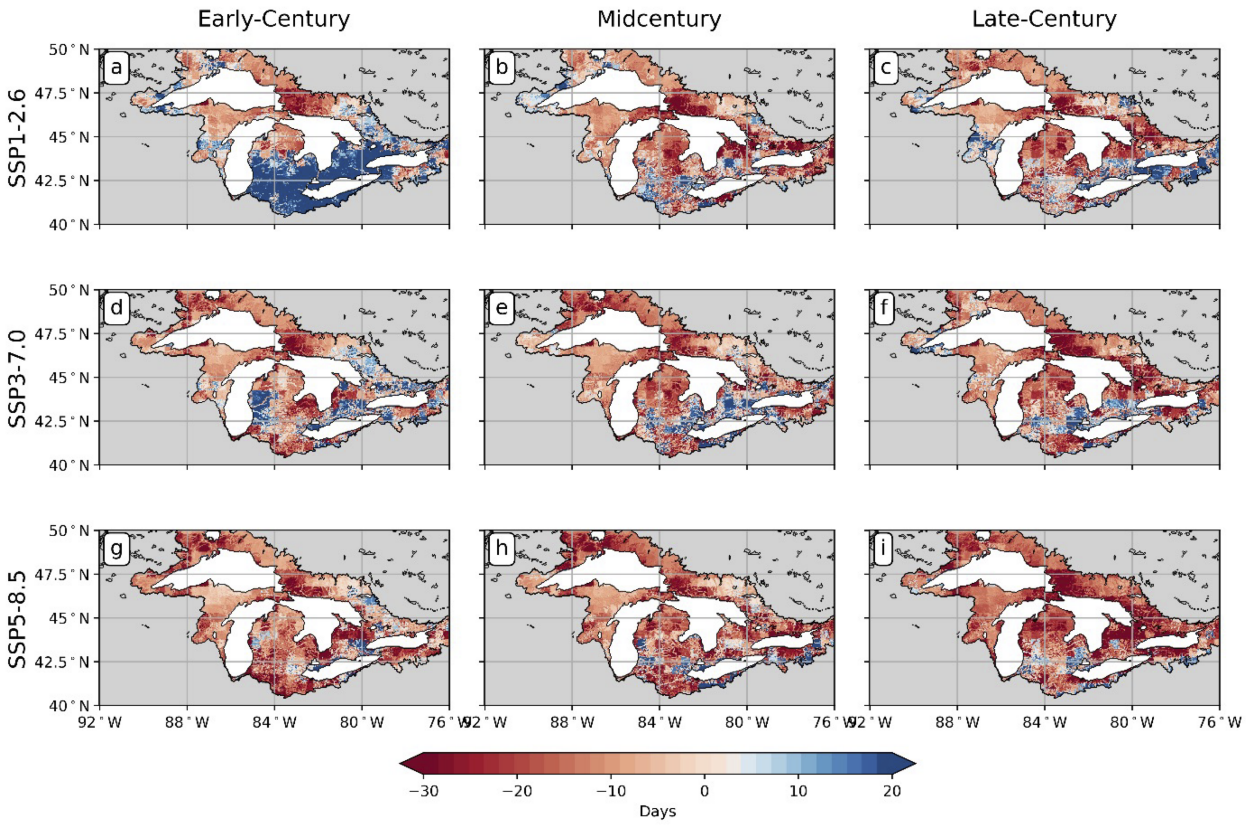

Figure 4.2 Maps of projected changes in peak flow timing.

Under SSP1, the southern portion of the basin could see an overall delay in peak flow timing by more than 2 weeks from the historical baseline period. Peak flows are earlier predominantly in the Northern portion of the basin and are less consistent in the Southern portion. In the early period (2025-2050), the peak flows in Southern portion of the basin (generally south of the 45th Parallel) are seen to be delayed by more than 10 days, as compared to the historical baseline. Whereas peak flows in the Northern potion of the basin (north of the 45th Parallel) occur on average 10 earlier in the Eastern portion of the Lake Superior sub-basin and 30 or more days earlier in the Western portion of the Lake Huron sub-basin. In the mid-century period (2050-2075), peak flows are shown to occur an average of 2 or more weeks earlier, and more than 30 days earlier in the Eastern portion of the Lake Superior sub-basin and Northwestern portion of the Lake Huron sub-basin. The southernmost parts of Michigan show a slight delay in peak flows, however. In the late-century

period (2075-2100), peak flows generally occur 10-30 or more days earlier as compared to the historical baseline period. The portion of the basin beneath the 45th parallel exhibits the same shift as most of the rest of the basin, with the exception of some of the southeastern parts of Michigan and the southern part of the Lake Ontario sub-basin.

Under SSP3, there are still some regions that exhibit a delay in peak flow, however this is far less than that of SSP1 and the magnitude of the shift is less as well. In the early period, western Michigan and much of the eastern portions of the basin show delays in peak flow timing by up to 10 days. However, most of the rest of the basin shows peak discharge timing occurring 7-10 days sooner than in the historical baseline period. Some areas show peak discharge occurring 30 of more days sooner than in the historical baseline period, notably the eastern part of Michigan's Upper Peninsula, Michigan's "Thumb" and Canada's Bruce Peninsula in Lake Huron. In the mid-century period, many of the areas that saw delays in peak flow timing now see them shift earlier than compared to the historical period, notably Western Michigan. Many of the areas that saw slightly earlier timing by 7-10 days now see much earlier timing by 20-30 or more days, notably in the northernmost portion of the region. By the end of the century, these patterns intensify. Most of the region sees a significant shift in peak flow by up to 30 or more days. Few areas, including Southeastern Michigan, see a delay in peak flows.

Under SSP5, nearly every cell exhibits a significant earlier peak flow timing, by more than a month in some places. Most significantly this occurs around Lake Huron and Lake Superior, primarily in western Ontario, Canada. In the early period, the majority of the basin sees peak flows 7-10 days earlier. Some areas are much earlier, including Northern and Eastern portions of the Lake Superior sub-basin, and the southernmost part of the basin in Michigan, Indiana and Ohio. Peak flows are shown to occur even early by the mid-century, approximately 20 days before historical average. Notably in the Lake Superior and Lake Huron sub-basins and in the Lower peninsula of Michigan. Further, by the end of the 21st century, under SSP5, nearly every portion of the basin sees peak flows occurring more than 20-30 days earlier.

Lower elevation areas, such as the eastern portion of Michigan's Upper Peninsula, are seeing

more dramatic earlier shifts in peak flow timing. These low-lying areas consistently face earlier peak flows due to slightly higher temperatures than surrounding areas, contributing to higher winter temperatures, more precipitation as rain rather than snow and higher rates of snowmelt. These areas also tend to collect more water due to the nature of their lower elevations. Similar results have been found by Regonda and Rajagopalan et al. 2004, who studied Seasonal Cycle Shifts in Hydroclimatology over the Western United States [55, 54]. Additionally, these results point to additional implications for infrastructure planning, flood management, and emergency preparedness in agricultural regions.

Peak flows are shown to shift across the basin under each scenario by the end of the century, by up to a month or more in some regions under all scenarios, particularly in the North and under SSP5. These shifts have important implications for water resource decision making, particularly for agriculture and infrastructure.

4.3 Surface Water Storage

Surface water storage (SWS) encompasses water accumulated on the soil surface or underground, water intercepted by vegetation, and water retained in depressions [41]. SWS is directly reflects the overall water balance of a region, affecting water availability for various uses such as agriculture, industry, and municipal supply [67]. SWS can serve as a buffer against droughts, making it essential to monitor and manage effectively in the face of climate change [6]. Changes in SWS can lead profound implications for both humans and natural ecosystems, especially in terms of agriculture [67].

Figure 4.3 shows the percent change of SWS mean over each period (2025-2049, 2050-2074, 2075-2099) under each climate change scenario (SSP1, SSP3 and SSP5) is depicted in each panel (a-i), respectively. The red shade represents a negative percent change, i.e. a decrease in SWS, while a blue shade represents a positive percent change, i.e. an increase in SWS. Note that the Great Lakes were not included in this analysis.

My results reveal a notable increase in SWS, particularly pronounced in scenarios SSP3 and SSP5 in the later parts of the 21st century. Notably, the westernmost points experience a substantial

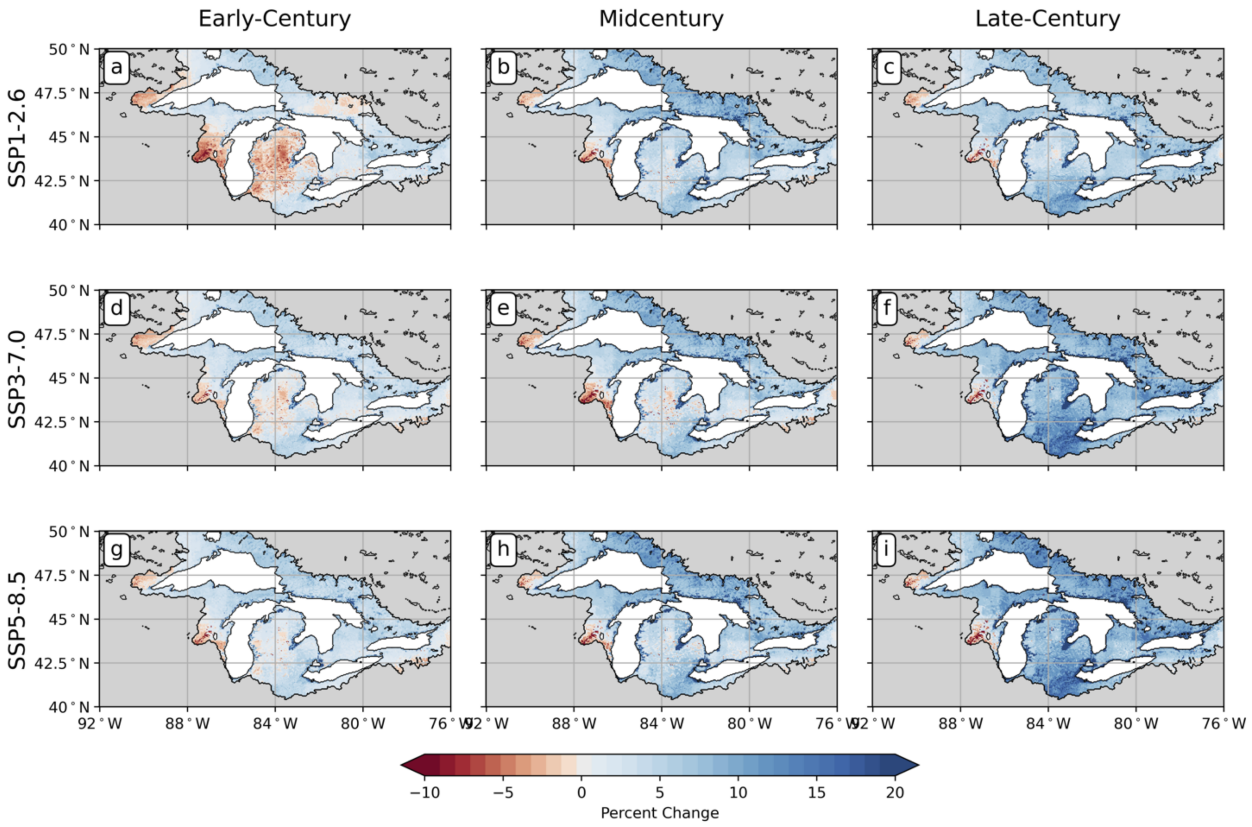

Figure 4.3 Projected maps of change in surface water storage.

decrease of up to 20% under all scenarios, intensifying over time. These changes are attributed to changes in the amount, type and timing of precipitation events and by increases in temperature throughout the basin [10, 17].

In the initial period (2025 – 2050), the GLB demonstrates slight change in mean SWS, indicated by light blue and light red colors in the figure. Under SSP1, a localized decrease of up to 20% is observed in Wisconsin and the Lower Peninsula of Michigan in the Early-Century period. This decrease consistently shows in inland Wisconsin across all future period and scenarios. This does change, however, in the Lower Peninsula of Michigan throughout the century and shows either no significance changes from the baseline period or increases.

It is also shown in figure 4.3 that the areas with the largest increase (up to 20% or more) are low-lying coastal areas and rivers near the Great Lakes, especially along the Eastern coast of Lake Michigan and the Northern coasts of Lake Huron and Lake Erie. This pattern first appears in the

Early-Century period, continues throughout the century and is consistent among all climate change scenarios.

SSP1 shows the smallest percent change compared to the baseline throughout the century. Conversely, significant increases are noted in the eastern and northern regions throughout the century, particularly pronounced in SSP3 and SSP5, especially in later periods (2050-2074 and 2075-2099). The southern portion of the basin, spanning Michigan, exhibits the most significant increase (> 20% in some areas) in the late century under SSP3 and SSP5. These results are consistent with the projected streamflow analysis of [21], who found that annual streamflow increased in all assessed rivers throughout the GLB throughout the century.

These changes are significant because increases in SWS can reflect increases in flooding, which can cause a decrease in agricultural yield, changes in market demand, and potential disruptions to supply chains that may affect the economic viability of agriculture in the region [45, 91]. Similarly, changes in water levels may affect water quality by influencing nutrient concentrations, sedimentation rates, and pollutant transport, which could also impact agriculture [50, 54].

Figure 4.3 reveals a general increase in mean SWS across the GLB under all climate change scenarios and in all periods. Such changes in SWS can have profound implications for both humans and natural ecosystems, especially in terms of agriculture and infrastructure [67, 60]. Heavy precipitation in the planting season, coupled with already nearly saturated soils, could lead to water logging, causing delays in planting [47, 64]. Or, if crops had already been planted, could lead to plant death [64]. Additionally, excess water in the growing could require farmers to implement water control devices. Increases in annual precipitation rates and extreme precipitation events, could add stress to dams and reservoirs, contributing to dam failure and extreme flooding [31]. Anticipating changes in SWS are essential to effectively manage water resources in the face of climate change.

4.4 Lake Water Levels

The water levels in the Great Lakes do not perfectly reflect the overall water balance of the basin [25, 41]. The Great Lakes water balance consists of components: runoff, precipitation, and

evaporation [25, 41]. Precipitation and evaporation, however, commonly balance each other out, because P and E are overlake processes [25]. Water levels in the Great Lakes historically have showed high amounts of fluctuations (CITE USACE). Commonly see several higher years in a row, followed by several lower years in a row [25]. However, in the past two decades or so, the fluctuations between these two extremes has accelerated – in 2014, the lakes saw the fastest rise in water level ever recorded [34].

Changes in water levels and water level fluctuations have significant implications on the environment, infrastructure, and water supply. For instance, high water levels and high fluctuations in water levels can contribute to coastal erosion, and high bank regions are -particularly vulnerable. Furthermore, water levels impact infrastructure, including dams, by reducing hydropower capacity [34, 60]. All of these impacts have crucial environmental, economic and societal consequences.

Figure 4.4 shows the historical and projected future lake water levels under climate change. The black line represents the historical lake water levels, the green, yellow and red lines represent SSP1, SSP3 and SSP5, respectively. The units for this figure are meters (m), depicting surface water elevation at one point in each lake. The points selected for analysis were closest to the points of the United States Army Corpse of Engineers' (USACE) water level monitors. Observed monthly water level data from these monitors spans back to 1918.

In the historical period, from 1971-2014, the lake water levels seem to consistently fall. Then, around the year 2040 in the future scenarios, the water levels begin to rebound and rise to levels above the historical peak of 1971. Lake water levels remain relatively consistent as compared to the historical period until approximately 2040, after which they begin to rise. There are several cycles of highs and lows throughout the rest of the century in each lake, however each lake shows an increase.

The figure shows that there were fewer and less extreme drops and rises in water level, and more in future period. This conveys the message of higher variation in lake water level in the future period as compared to the historical. Interestingly, the most variation occurs under SSP1, alternating from peaks to valleys in the shortest amount of time, while the other two scenarios

show the largest overall increase, they show much less variation. The fastest increase and decrease in water level also occurs under SSP1, throughout the early 2030s. This change is faster than anything seen throughout the historical period. This is reflected by the least amount of change in precipitation and temperature, both of which are dominant contributing factor to the Great Lakes water balance components runoff, precipitation, and evaporation. SSP5 shows the least amount of variation, but a consistent increase in all of the lakes.

In particular, Lake Superior shows the least amount of variation under all scenarios, and, by the end of the century, the water level is roughly the same. Lake Superior is the largest lake, it is also the deepest and the coldest. Historically, it has also maintained the most consistent water levels, and this proves to remain true into the future periods. The other lakes, which are shallower, warmer and generally show more variation in water level historically, have a consistently increasing trend in water level throughout the century.

Lake water levels and variation in lake water levels consistently rise in all of the lakes under all climate change scenarios by the end of the 21st century. Notable increase by late century under SSP3 and SSP5 compared to SSP1 in all lakes by the end of the century. Of these, SSP5 show the largest increase throughout the 21st century. These increased water levels and intensified extreme events will lead to increased variation in river discharge and lake shoreline levels [33]. During low times, beaches are much longer and wider than during high times, where beaches are virtually non existent [48]. Recently, shorelines have reached historic highs and lows, we saw historically low levels in 2013; and then just 7 years later, we saw extreme high levels [48]. These trends, constantly alternating between highs and lows, are anticipated to continue under climate change. Many of these areas are high banks, where the dunes naturally rise tens to hundreds of feet above the water [88]. These coastal areas, particularly high banks, are highly vulnerable to erosion, especially with these conditions intensifying under climate change [88]. These changes in lake water levels could have adverse impacts on the local economy and environment, especially on man-made infrastructure including roads, beaches and dams, and could alter recreation and infrastructure management strategies [60].

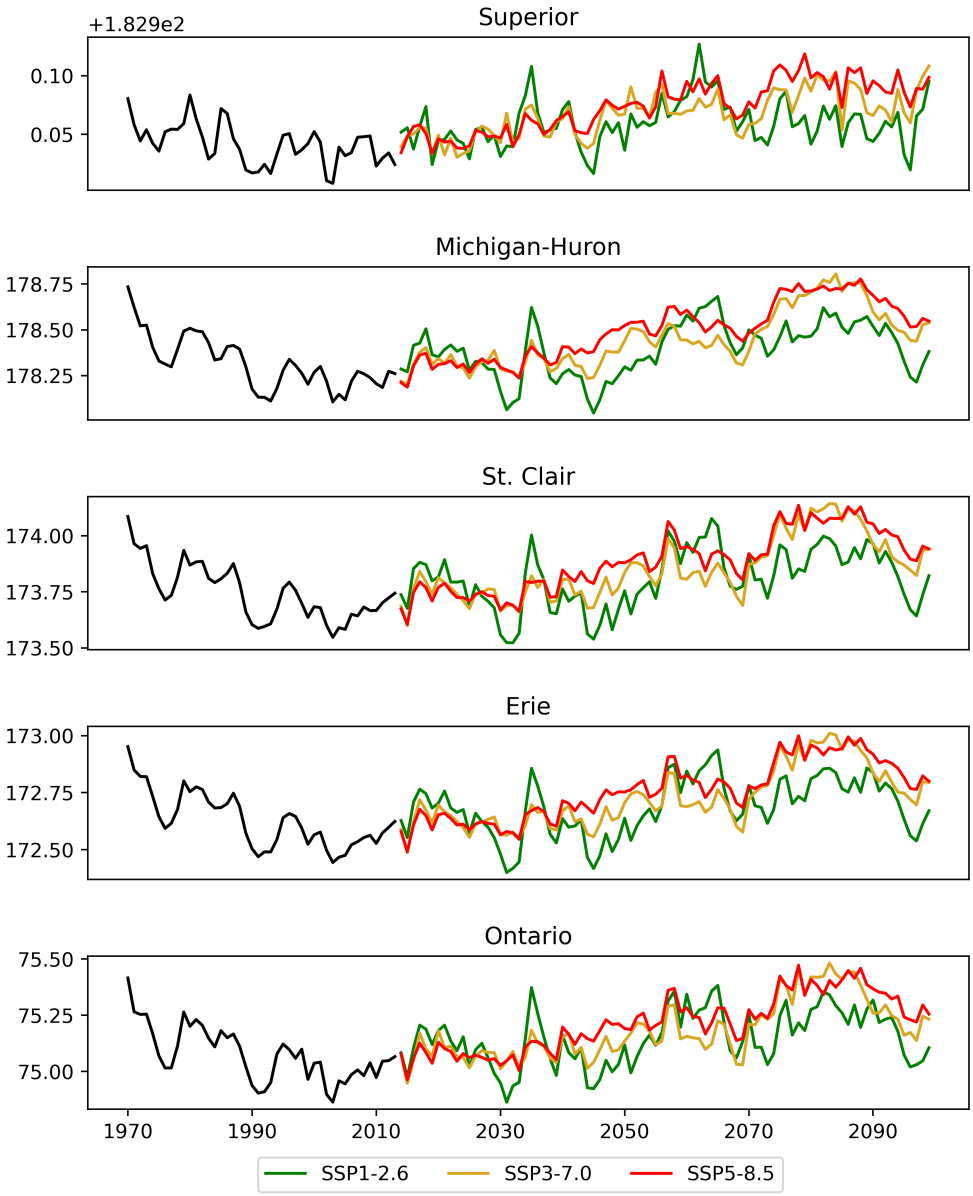

Figure 4.4 Historical and projected lake water levels.

4.5 Hydrological Extremes

Devastating floods have become larger and more frequent due to climate change. The Intergovernmental Panel on Climate Change (IPCC) has found that climate change has "detectably influenced" factors like rainfall and snowmelt that contribute to flooding [89]. A warmer atmosphere holds and dumps more water, leading to heavier precipitation events that are projected to increase by 50% to 300% in the United States [85].

One recent example of devastating floods exacerbated by climate change was the 2020 dam failures in Midland and Edinburg [38]. An extreme rainfall event caused the failure of two massive dams and caused widespread damage, and disruption to critical infrastructure [31].

Therefore, to mitigate the effects of these increasingly common and severe floods, it is crucial to anticipate such events and prepare through measures like improved flood forecasting and early warning systems, as well as maintenance and scheduling of dams and other flood control infrastructure [31]. Proactive adaptation and resilience-building efforts will be essential to protect communities and critical assets from the growing flood risks posed by climate change.

A "10-year flood" is a flood with such a large magnitude that it has a 10% chance of occurring any given year. It is likely to happen once in 10 years, so 10 years is the return period. However, it is not guaranteed to happen, or may happen more than once. Similarly, a 25-, 50-year and 100-year flood has a return period of 25, 50 and 100 years and a 4%, 2% and 1%, chance of happening in any given year, respectively. To calculate the magnitude of one of these floods, first examine the historical data. Find the maximum value, its return period – which is the length of the dataset in years – and the standard deviation of the dataset. Then using equation equation 2.3, calculate the magnitude of the flood with the desired return period. To calculate the frequency of these events in the future period, I calculated the magnitudes of each of these return periods for each cell in the basin (40,000 cells total). Then, using the future projection data, I calculated the number of occurrences of these magnitudes in each cell each year. Then I took the average across all cells. Because of this, this calculation is a generalization across the basin, so some areas may see more floods than others, especially river floodplains and coastal areas.

Figure 4.5 shows the projected frequency of 10-, 25-, 50-, and 100- year floods in the GLB throughout the 21st century under the three climate change scenarios. Green, yellow and red depict scenarios SSP1, SSP3 and SSP5, respectively.

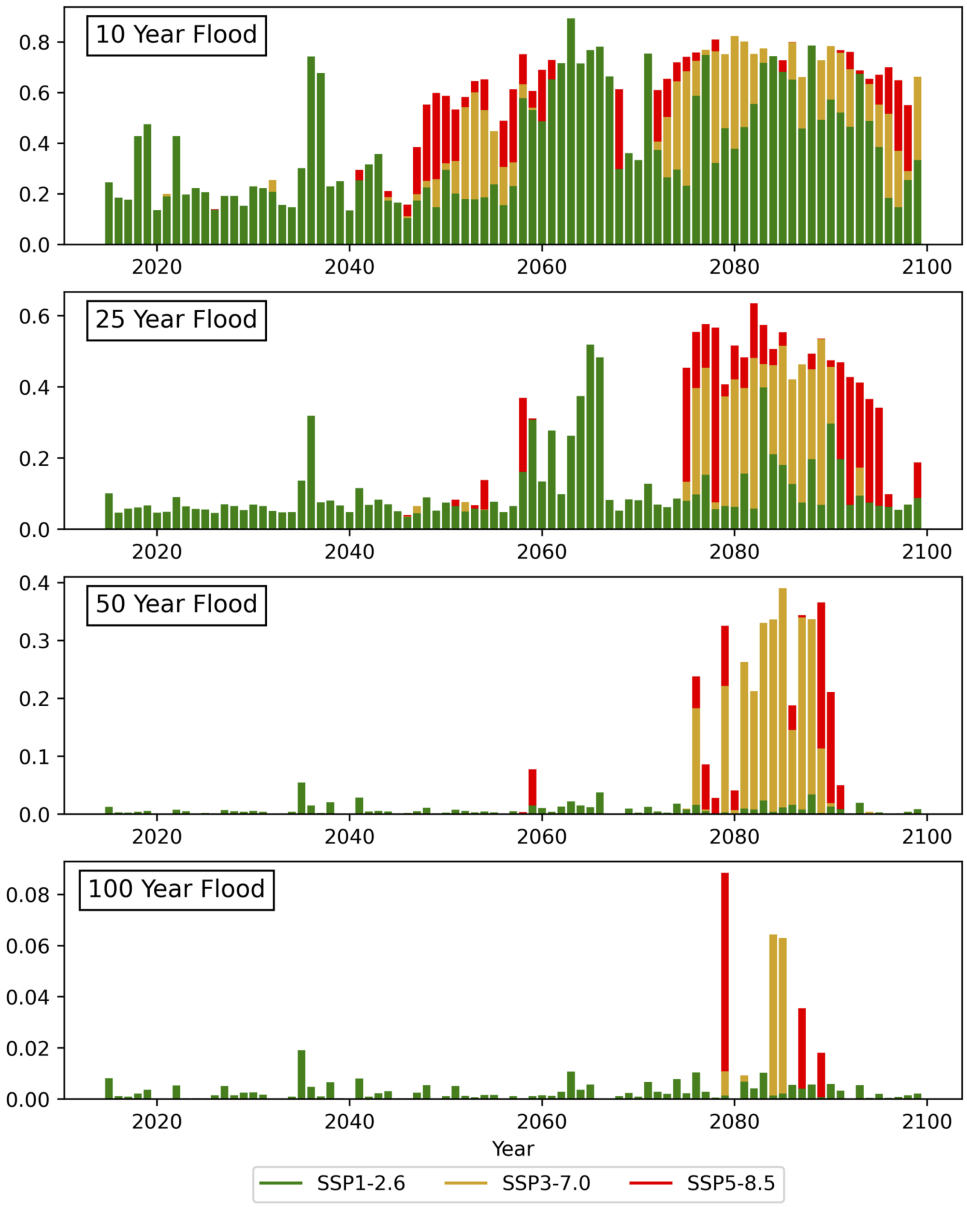

Figure 4.5 Changes in extreme flood frequency under climate change.

Under all scenarios, in the early century period, the number of 10-year floods changes significantly from the historical period. On average, the basin faces .2 10-year floods per year, which would be double the amount as compared to the historical period. SSP1 shows the highest number of floods in this period, especially during certain years in the early 2020s. SSP3 and SSP5 are largely the same until the mid-century period. In the mid-century period, the number of 10-year floods under SSP5 increases dramatically, by a factor of 6x, and remains this way for several

decades. A similar trend happens, but later, under SSP3, and even later under SSP1. By the late century period, the number of 10-year floods has increased by a factor of 7x on average under SSP3 and SSP5. SSP1 also shows an increase in 10-year floods by a factor of 5x but shows overall fewer. Under SSP1, SSP3 and SSP5, the number of 10-year floods increases by .4%, .75%, and .88% per year, respectively. By the end of the 21st century, under all scenarios, the GLB could face up to .48-.71 10-year floods per year or more, a factor that is 8x higher than the historical period.

The number of 25-year floods does not change significantly as compared to the historical period under any of the scenarios until end of the early century period, even then only under SSP1 do the number of occurrences increase only in certain years. In the mid-century period, the number of 25-year floods increases by a factor of 4x under SSP1, 1.5x under SSP3 and 2x under SSP5. By the late century period, the number of 25- year floods increases up to 3-10x under all scenarios in the late century period, and this increases the most under SSP3 (7x) and SSP5 (10x). Under SSP1, SSP3 and SSP5, the number of 25-year floods increases by .1%, .32%, and .52% per year, respectively. By the end of the 21st century, under all scenarios, the GLB could face up to .15-.41 25-year floods per year or more, a factor that is 8x higher than the historical period.

The number of 50-year floods does not change significantly as compared to the historical period under any of the scenarios until end of the early century period, even then only under SSP1 do the number of occurrences increase only in certain years. However, by the late 21st century period, 50-year floods are much more likely, especially under SSP3 and SSP5. Under SSP1, SSP3 and SSP5, the number of 50-year floods increases by .004%, .15%, and .16% per year, respectively. And, by the end of the 21st century, under all scenarios, the GLB could face up to .11 50-year floods per year or more, a factor that is 5x higher than the historical period.

Lastly, the frequency of 100- year floods could increase 9x by the end of the century under SSP5. Under SSP1, the number of 100-year floods could double throughout the century, with a maximum annual average number being 0.02. This figure is 3x higher under SSP3 and 4.5x higher under SSP5. Under SSP1, SSP3 and SSP5, the number of 100-year floods increases by .0009%, .008%, and .007% per year, respectively.

It is shown in Figure 4.5 that the frequency of 10-, 25-, 50- and 100- year floods increases under all climate change scenarios throughout the rest of the century. By the end of the 21st century, on average the GLB could see approximately 2-8x as many 10 year, 3-10x as many 25-year, 5x as many 50-year and 2-9x times as many 100-year floods each year as compared to the historical period. The impacts of these extreme flood events could be devastating to the GLB, impacting all aspects of life in the basin. Extreme floods cause great damage to infrastructure, leading to dam breaks and failures, erosion of bridges and other critical structures, which would cost millions of dollars to repair. Large floods could also cause fields to flood crops to die, potentially leading to food shortages and regional economic issues.

CHAPTER 5

IMPLICATIONS FOR AGRICULTURE

The GLB is a critical agricultural area. Shown in Figure 1.2 in Chapter 1 is a land use/land cover map of the basin, blue is water, red is majorly developed areas, green is forest, yellow is agriculture – agriculture occupies much of the southern portion of the basin. In total, agriculture covers approximately a quarter of the total land area. This chapter builds upon the results of the previous chapter by providing a detailed analysis on the impacts of climate change on water availability in the GLB. By investigating changes in the timing and magnitude of maximum flows and the occurrence and magnitude of floods in the planting season, and examining changes in the spatial and temporal occurrence of growing season droughts, we can begin to understand the potential consequence impacts on agricultural practices in this region.

In a 2010 study conducted by the United States Environmental Protection Agency (US EPA), a correlation between extreme hydrological and meteorological events and annual corn yields in bushels per acre was found. The researchers concluded that both floods and droughts historically have been linked to lower yields [91, 64]. Increases in floods, specifically during the planting season, cause waterlogging, which could lead to delays in planting [47, 64]. However, yields decrease significantly if planted too late. Corn yields in particular, after May 15 [58]. Conversely, increases in growing season drought frequency and intensity could limit the amount of water for plant growth [91].

Historically in the GLB, as shown in Figure 3.3 high flows occur in March, April and May (MAM) (spring) – typically peaking in March –followed by low flows in July, August and September (JAS) (summer). Currently, planting season typically begins around the middle of April, when freezing temperatures are anomalous and flows are still high, allowing plenty of water for plants. Then, the growing season begins around the end of planting season, June at the latest in some areas – water availability decreases throughout the summer; some areas require irrigation for maximum yield. Lastly, the harvest season begins after the end of growing season. In this study, the timing of planting and harvesting seasons were taken as the earliest to latest usual dates for each according to

United States Department of Agriculture Usual Planting and Harvesting Dates for U.S. Field Crops, 1997, which analyzed historical planting and harvest dates data from a period of 105 years (1895 – 2000) [55]. The beginning and ending dates represent when planting or harvesting is about 5% or 95% completed, respectively. Thus, the optimal planting season was considered to be April 22 – June 15, as planting after this day will decrease crop yield significantly [59]. The harvest season was considered to be September 24 – December 1. Similarly, the growing season was considered to start from the earliest planting date to the latest harvest date and was defined as May 28 – December 1. Generally, the growing season throughout the basin varies by 1 month but is mostly consistent throughout the agriculturally dominant regions [39]. Figure 5.1 shows a timeline of the planting, growing and harvest seasons in the basin. Under climate change, planting and growing seasons may be altered, so farmers may have to adjust their agricultural practices, such as irrigation schemes, due to projected changes in precipitation and temperature throughout the year.

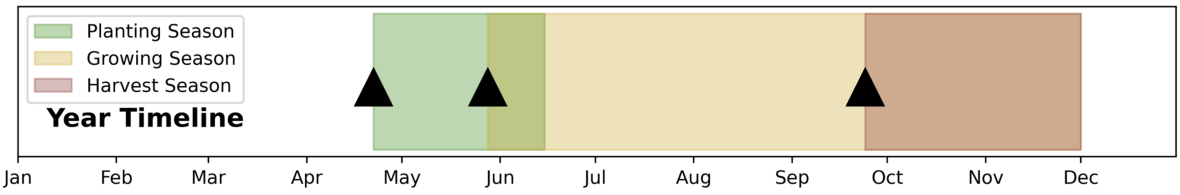

Figure 5.1 Timeline of the typical planting, growing and harvest seasons in the GLB.

Maximum flow holds significant importance for agriculture due to its influence on both magnitude and timing of water availability. If there is too much water in the planting season, fields could be waterlogged, forcing farmers to delay planting [47]. Floods during the growing season can wash away seeds, drown crops, and disrupt crop development, impacting agriculture practices [47, 64]. Conversely, if there is not enough water in the planting season, farmers must irrigate their crops [91]. Furthermore, droughts can lead to soil moisture deficits, reduced water availability for irrigation, and crop failures, resulting in decreased yields and economic losses for farmers [91]. Extreme events such as floods and droughts during planting or growing stages can lead to yield losses and financial setbacks for farmers [64, 91]. Managing risks through warning systems,

zoning, and resilient farming practices can help farmers adapt to these extreme events and enhance agricultural resilience in the face of changing climatic conditions.

5.1 Floods in Planting Season

The planting season is the time period during which farmers sow seeds or transplant seedlings into the soil to initiate crop growth. It typically occurs after the day of last frost in the GLB. In this study, the planting season was taken to start on April 22 and end on June 15 [59].

5.1.1 Changes in Maximum Discharge Timing, Occurrence and Magnitude

The timing and magnitude of annual planting season peak discharge is important for agriculture because it informs decisions on planting dates, water availability for irrigation, flooding and risk management [63]. During periods of high flow, excess water may cause flooding, leading to crop damage, soil erosion, and infrastructure destruction [93]. These peak flows are projected to shift earlier in the year (up to a month), potentially causing flooding and forcing farmers into delaying planting or implementing other flood-prevention measures such as tile drainage systems or dams [16]. Understanding changes in maximum flow timing and magnitude under climate change, helps farmers plan for planting season by examining water availability and usage, and minimize risks.

Figure 5.2 shows spatial and temporal trends in the timing and magnitude of annual planting season peak flow under each climate change scenario. The decadal trend in mean day of maximum discharge over the projected 75 year period (2025-2099) under each climate change scenario (SSP1, SSP3 and SSP5) is depicted in each panel (a-c), respectively.

Under SSP1, the decadal trend in peak flow timing is less than 1-2 days per decade in the most of the basin. However, in the Northern portion of the basin; north of the 45th parallel, and the very Southern portions of the basin; in Northern Ohio and New York, there is a slight trend of earlier peak flow timing, and throughout the Lower Peninsula of Michigan there is a delay in peak flows. These patterns intensify with each climate change scenario, notably the magnitude of the earlier shifts in the northern and southern-most portions of the basin increase to up to 2 days per decade.

The timing of maximum discharge in agricultural areas suggests that the peak flow event is undergoing slight shifts in timing. Under SSP1, the decadal trend in peak flow timing is seemingly

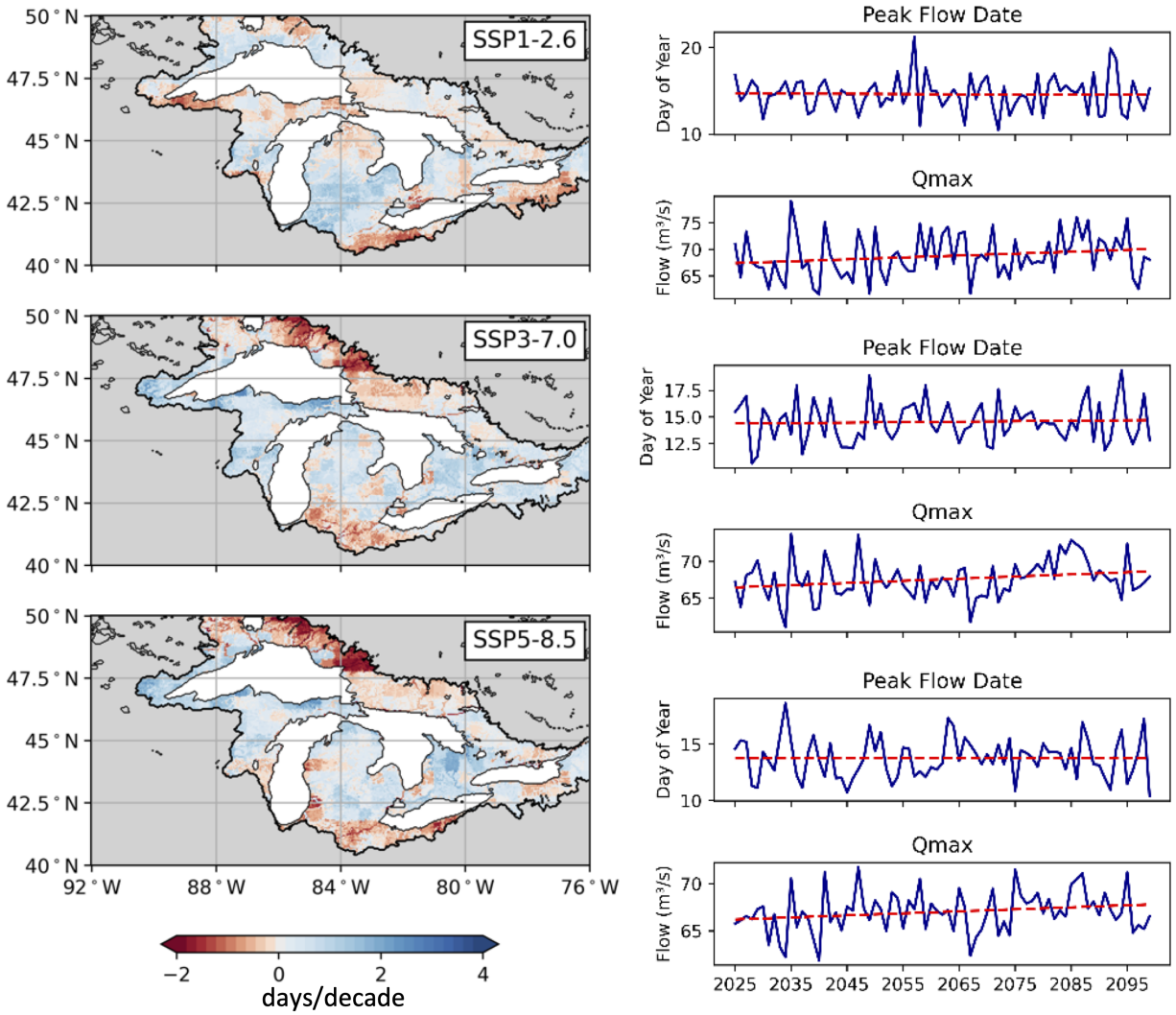

Figure 5.2 Maximum flow timing and magnitude in the planting season.

insignificant, only 1-2 days per decade in the most dramatic regions. However, 2 days per decade for 5 decades is 10 days, which is significant in terms of the planting season. Under SSP1, much of the basin shows a slight delaying trend in peak flow timing, meaning farmers may have to delay planting. If planting is delayed past the optimal planting season, then crop yields decrease dramatically with each additional day of delay [61, 59].

Further, the increasing maximum discharge implies a heightened risk of extreme flooding events, particularly under SSP1 and SSP5 scenarios. This could have substantial consequences for infrastructure, crop damage, and overall safety in agricultural regions.

5.1.2 Changes in Planting Season Flood Magnitude and Occurrence

Floods hold significant importance for agriculture as well because the extent of inundation and volume of water can affect agricultural land. High-magnitude floods can lead to soil erosion, crop damage, and infrastructure destruction, impacting agricultural productivity [93]. If there is too much flooding, farmers may need to implement mitigation measures such as flood-resistant crops, soil conservation practices, and proper land use planning to minimize the adverse effects of flooding. Flooding during planting or growing stages can drown crops, wash away seeds, and disrupt crop development, leading to yield losses and financial setbacks for farmers.

Figure 5.3 presents the spatial and temporal changes in flood magnitude across the GLB. SSP1 showed increases in mean flood depth in the southwestern portion of basin early on, a mid-century decrease, and late-century increases, particularly in in-land, agriculturally dominated areas. The small sub-panels display the in-land, agriculturally dominated areas under the same scenarios during the same periods. A red shade represents a decrease in mean annual spring flood depth, and a blue shade represents an increase in mean annual spring flood depth. The line graphs at the bottom shows the annual mean basin wide flood depth. For both, the historical scenario is displayed in black, while the projected climate scenarios SSP1, SSP3 and SSP5 are displayed in green, yellow and red, respectively. Over each projection is a corresponding trendline, shown as a dashed line in the same color as the scenario. Here, flood occurrence was determined to be the total number of days in the planting season where flood depth was greater than 0 in each cell, then the mean across the basin was taken and is displayed in the bottom left panel. Flood depth was determined to be the mean annual growing season flood depth across the basin, and is displayed in the bottom right panel.

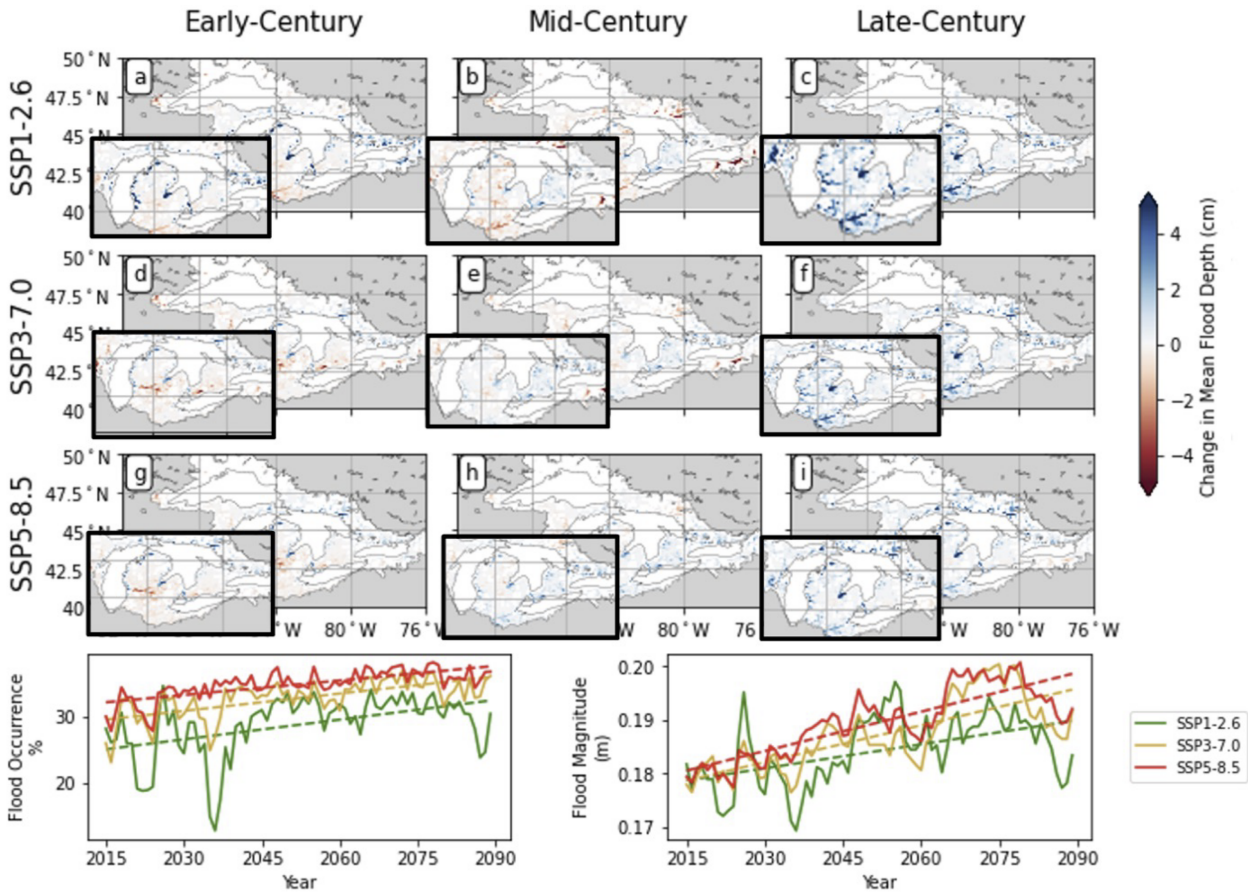

Figure 5.3 Planting season flood occurrence and magnitude.

As the GLB transitions to warmer winters, increased winter precipitation and more intense rainfall is anticipated to elevate flooding across the GLB [16]. First, the top panels show change in mean flood depth throughout the growing season. As shown, there is not a large change early on, but even a few cm/inches can damage crops. The largest change occurred in late century under SSP1; maybe rainfall/snowmelt is more spread-out throughout the season, whereas in SSP3 and SSP5 it occurs with higher intensity, all at once. Most significantly, flood depth increased in coastal and floodplain areas, especially in the late century period. The northern portion of the basin, including the UP of Michigan showed a decrease in mean spring flood depth throughout the century under all scenarios. SSP3 exhibited diverse patterns, with notable decreases in the UP of Michigan and Wisconsin. SSP5 displayed similarities to SSP1 and SSP3 but with higher magnitudes.

Our results reveal a heightened magnitude and frequency of floods, marked by a consistent increase in both flood depth and occurrence under all climate change scenarios, but most significantly under SSP5. This aligns with the overall rise in water balance as indicated in section 3.2.2. and previous findings [10, 17]. This is predicted to contribute to seasonal flood magnitude and occurrence, posing challenges to farmers.

Our results show that flood depth was shown to consistently increase across scenarios, with the highest increase under SSP5, and the smallest occurring under SSP1. While soil water storage is not explicitly calculated/demonstrated in this study, it is highly relevant to the discussion of flood events in relation to agriculture. One study describes changes in spring soil water storage as increasing by up to 5% in the spring, and decreasing up to 9 percent in the fall, varying spatially, and concludes that "wetter springs could make agricultural planting difficult and the potential for flooding more likely" [9]. These results contribute to a better understanding of the potential risks associated with climate change-induced changes in spring floods. The results are crucial for farmers and agricultural communities, particularly those in the southern portion of the basin, which showed the most significant increases in mean annual flood depth. Changes in flood magnitude during the planting season can directly impact crop yields, affecting food production and economic livelihoods. The identified shifts in flood occurrence can guide decision-making for planting strategies and crop selection. Overall, flood depth and occurrence increase under all scenarios by the end of the 21st century.

5.2 Droughts in Growing Season

Growing season droughts have significant implications for agriculture. Droughts occurring during key growth stages, such as germination, flowering, and grain filling, can stunt crop growth, reduce photosynthesis, and limit nutrient uptake, leading to yield losses and decreased crop quality [91]. They can also lead to soil moisture deficits, reduced water availability for irrigation, and crop failures, resulting in decreased yields and economic losses for farmers [91]. Effective drought monitoring and early warning systems enable farmers to anticipate drought events, adjust planting dates, and implement drought-tolerant crop varieties and management practices to minimize yield

losses and maintain agricultural productivity during periods of water scarcity [99].

Analyzing summer drought magnitude and frequency in the GLB under climate change is crucial because it has significant implications for agricultural production and water resource management [99, 91]. As climate change exacerbates drought conditions, understanding the specific impacts on agriculture is essential for developing strategies to ensure food security and sustainable farming practices.

In this study, growing season hydrological drought was examined using the Streamflow Drought Index and was calculated using equation 2.4 [70]. The growing season was considered May 31 – September 1, as defined previously and shown in TIMELINE FIGURE. Figure 5.4 shows the drought frequency, magnitude and occurrence in the GLB through the year 2100 under each climate change scenario (SSP1, SSP3 and SSP5) is depicted in each panel. The line graphs on the left display the annual mean percent of summer drought days of each state of drought, 0 (non-drought) through 4 (extreme drought), as defined previously in 2.3, with increasing severity from top to bottom. The drought state was determined using 2.3. Since a positive or zero drought index indicated a non-drought state, the occurrence of any negative drought index was counted as a drought occurrence. The historical scenario is displayed in black, while the projected climate scenarios SSP1, SSP3 and SSP5 are displayed in green, yellow and red, respectively. Over each projection is a corresponding trendline, shown as a dashed line in the same color as the scenario. The maps on the right show the change in the mean number of drought days in the projected period as compared to the historical period. The number of drought occurrences in the growing season was recorded. The average for the historical period and the future periods were then taken. A red shade represents an in the number of drought days, and a white shade represents no change.

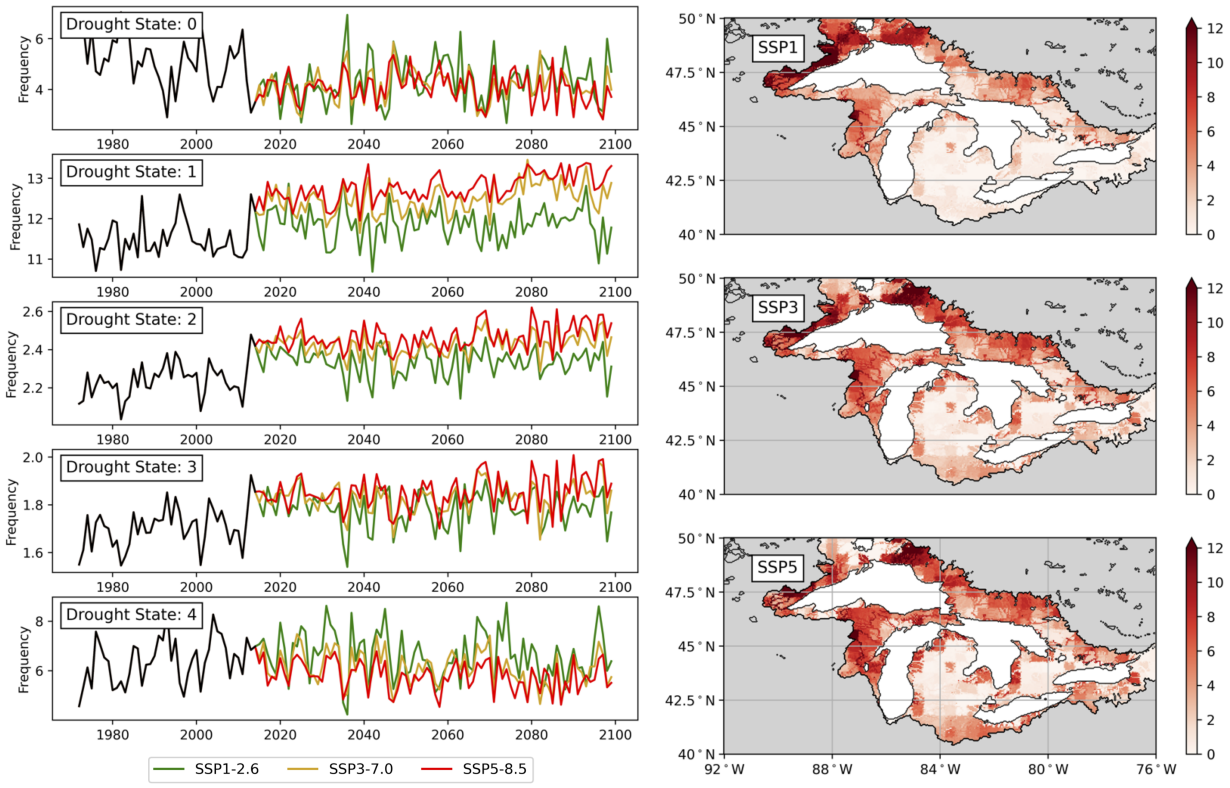

Figure 5.4 Growing season drought frequency, magnitude and occurrence.

In terms of drought magnitude, historically, there has been a mix of each of the drought states throughout the season. In the future, it appears that the number of total drought days does not change or decreases slightly. SSP1 showed the highest variation in the number of non-drought days – state index of 0 – but no consistent, significant trend was observed in the data. Under SSP1, mild drought (state 1) is shown to decrease slightly. SSP1 saw fewer state 2 and state 3 droughts, as compared to SSP3 and SSP5. SSP1 also showed the highest number of extreme droughts as compared to the other scenarios, however these decrease slightly through the century. There was a slightly higher occurrence of state 4 droughts throughout the century as compared to SSP3 or SSP5, but this was not different from the historical period. Overall, drought occurrence was not shown to change significantly throughout the century under SSP1, however, in general, the magnitude tended to become more severe. On the other hand, under SSP3 and SSP5, mild drought is increasing while severe drought is decreasing. SSP3 showed a slight decrease in the number of state 4 droughts and

an increase in state 1 droughts by the end of the century. SSP3 showed more droughts of states 1, 2 and 3 as compared to SSP1 but less as compared to SSP5. SSP5 showed a similar pattern in terms of drought state occurrences, but higher magnitude. These results are inconclusive because there the results are relatively inconsistent and show a completely different trends between scenarios. These changes could be due to changes in rainfall patterns; as we see a larger increase in surface water storage under SSP5 than SSP1. Perhaps more erratic rainfall patterns contribute to different types of droughts under the different scenarios.

The right figure shows a map of the change in number of drought days in each cell throughout the entire future period as compared to the historical period. Drought occurrence did not vary among scenarios as much, which as was expected. Under SSP1, the southeastern portion of the basin does not see a large change in drought days, however the northern and northwestern portions see anywhere from 6-12 more drought days per year on average. Under SSP3 and SSP5, this pattern is similar, except more of the basin sees more drought days. Spatially, the northern and northwestern portions of the basin saw the highest increase in number of drought days by up to 12 or more by the end of the century as compared to the historical baseline period. Changes in growing season droughts vary both spatially throughout the basin and by state, depending on which scenario is considered. Changes in planting and growing season flows could require infrastructural changes including increasing commission of dams and the usage of irrigation. Irrigation can help mitigate low flows during the growing season, while dams can help moderate extreme events, including both floods and droughts, as they moderate high and low flows. Dams are also commonly used to hold water for irrigation. In the GLB, one of the most common purposes of dams is for irrigation Figure 1.3.

Figure 5.5 shows the agricultural regions of the basin in orange, and the irrigated portions of these areas in dark grey. The bar charts represent the total irrigated and rain fed land proportion vs. their respective economic contributions. As shown in the grey colors of the bar graphs, only 8% of the agricultural land is irrigated; but these crops are specialty crops such as apples, alfalfa and other expensive crops [79, 2].

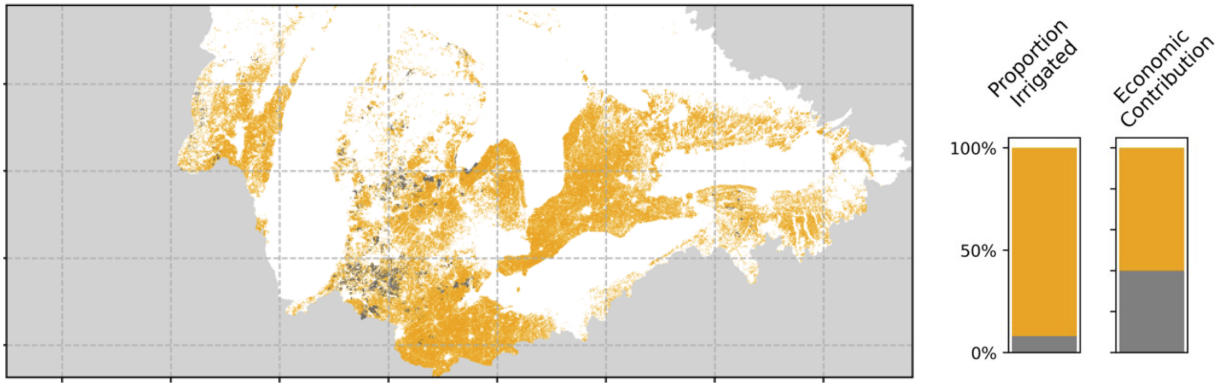

Figure 5.5 Agricultural and irrigated land in the GLB, bar charts of the land area and the economic contributions of each.

In summary, droughts' magnitude and timing significantly impact agriculture, particularly during the growing season, by affecting soil moisture availability, crop water requirements, and yield potential. Implementing proactive drought management strategies and adopting climate-resilient agricultural practices can help farmers adapt to drought conditions and sustainably manage water resources to ensure food security in the GLB.

CHAPTER 6

IMPLICATIONS FOR INFRASTRUCTURE

Climate change causes extreme events to intensify, exasperating local infrastructure [54]. In May of 2020, the Edinburg/Midland Dam failure was induced by torrential rains [38]. This devastating event was partially caused by dam mismanagement [38]. Such extreme flooding is anticipated to become more and more frequent under climate change [42]. These floods stress infrastructure, cause agricultural losses, and cause millions or billions of dollars in damage [42, 47]. This chapter builds upon the results of Chapters 3 and 4 by examining changes and trends in extreme flows throughout the basin, specifically at the locations of dams.

6.1 Trends in extreme flows

Figure 6.1 shows the basin wide trend in annual maximum and minimum discharge in m3/s for both the historical and future periods under the three climate change scenarios.. The historical period is included and is depicted in black. The projected period is shown under each of the three climate change scenarios, SSP1, SSP3 and SSP5, which are depicted in green, yellow and red, respectively. Over each projection is a corresponding trendline, shown as a dashed line in the same color as the scenario.

Peak annual discharge throughout the basin decreases by the end of the 21st century. Historically, basin wide discharge was around 8.5 m3/s with a maximum of 10 m3/s and a minimum of 7.5 m3/s. In the projected period, all scenarios show a slight decrease in annual maximum flow as compared to the historical period. SSP1 shows the highest amount of variation under SSP1, varying by more than 10% interannually. It appears to decrease slightly until 2040, then increase slightly for a few decades until 2060, and then remains relatively consistent for the rest of the century with another gradual increase in the later period (2080-2100). SSP3 shows the overall least trend throughout the century, as well as the second least amount of variation. SSP5 shows both the least amount of interannual variation and the largest overall decrease in maximum discharge.

Annual basin wide minimum discharge increases by 10% or more under each scenario, most notably under SSP5. Under SSP1, there is a high amount of variation in minimum flow, but this

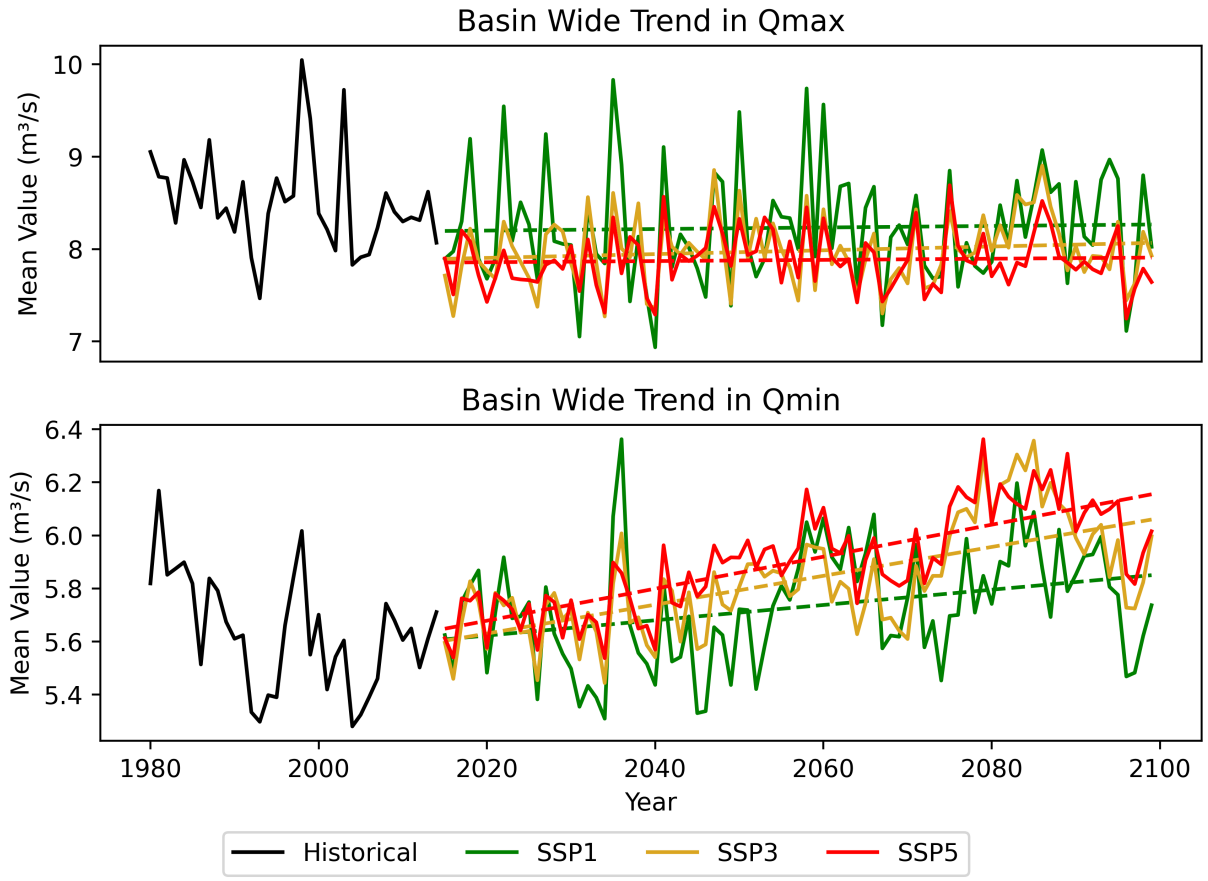

Figure 6.1 Annual maximum and minimum discharge.

scenario shows the least overall increase. Under SSP3, there is a slight increase in minimum flow and the second highest amount of variation. Lastly, under SSP5 there is the highest increase, and the least amount of variation in basin wide annual low flow. Overall, there is a gradual increase in basin wide mean low flow and there is also a high amount of interannual variation in minimum discharge as well. Such changes in minimum and maximum flows under climate change could increase the risk for dam failures in the future.

6.2 Trends in maximum flow at dams

My original research interest was in dam infrastructure in the GLB. Particularly, dam failures and breaks after the 2020 dam failure in Midland, Michigan. However, over time, my research interests changed and I discovered that agriculture is more pressing issue – however, future analysis

would focus on dam impacts. Included here is a brief touch on the topic of climate change impacts on dam infrastructure in the GLB. Another future research interest would be flooding issues in coastal areas, and implications of climate change on other infrastructure including roads and bridges.

Dams break or fail due to excessive inflows of water from heavy rainfall or rapid snowmelt, called hydraulic overloading [31, 60]. This water exceeds the dam's capacity, leading to overtopping, where water flows over the dam crest, potentially causing erosion or failure [31]. Cracks, leaks, or weaknesses in the dam structure may develop over time, increasing the risk of failure under hydraulic loading conditions [31, 83, 60]. Additionally, improper operation, inadequate monitoring, or failure to address warning signs of potential problems can contribute to dam failures [31]. When a dam breaks, water is released rapidly downstream, resulting in flooding, property damage, loss of life, and environmental destruction [31, 60]. Dam failures are rare but can have catastrophic consequences, therefore design, inspection, and risk management are critical to ensure safety and reliability.

Figure 6.2 shows 2 columns of maps of the GLB, where each triangle point is a dam.The left is overall linear trend, slope is given in cubic meters per second per year throughout the 85 year future projection period. Right is annual percent change in discharge through the same time period. Top, middle, and bottom panels represent SSP1, SSP3, and SSP5, respectively.

The figure on the left shows decadal mean change in annual discharge at each dam in the GLB. These values were normalized to the flow in each river and is measured in percent. Southern dams (below the 45th parallel) show the most pronounced increase in discharge (relative to their respective historical discharge) by up to 10% per decade under each scenario, while northern dams face a decrease in discharge by up to 10% per decade under each scenario. Under SSP1, this change is the least and it is mostly dams in the lower peninsula of Michigan that face alterations in extreme peak flows, with some in northern Ohio, and New York also experiencing the same changes, to a lesser degree. Under SSP3, these dams that faced changes under SSP1 face more intensified changes. Additionally, dams in the upper peninsula of Michigan and northern Wisconsin also face a decrease in peak flows, by up to 10% per decade or more. Lastly, under SSP5, these spatial

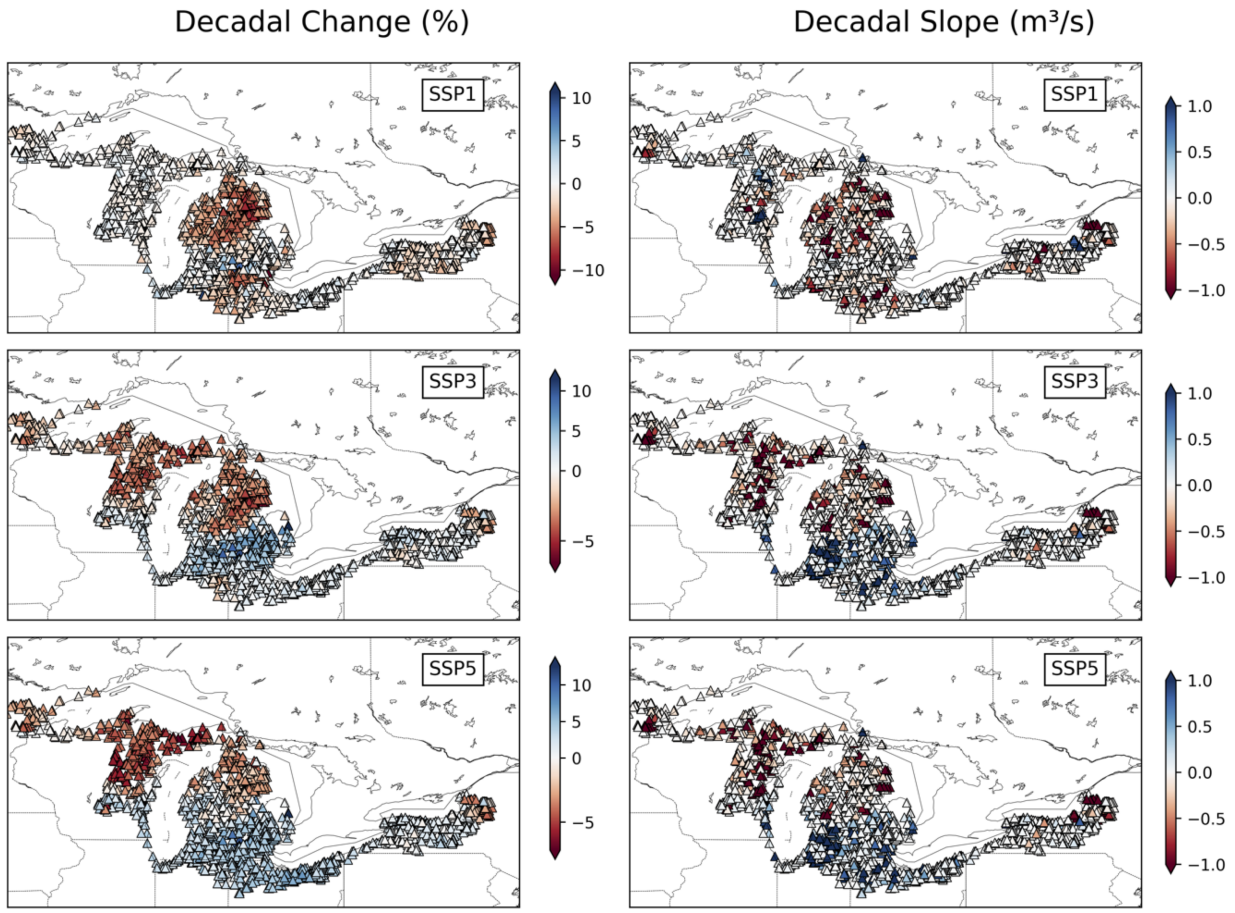

Figure 6.2 Change in extreme flows at dams.

patterns in high flows continue and are somewhat intensified, especially in the southern portion of the basin, where increases in high flows are more wide spread into northern Ohio.

The panels on the right shows overall decadal slope of annual maximum discharge. This figure is able to highlight the large dams on large rivers and give more detailed locations of which dams could be most highly vulnerable to the changes in maximum discharge, particularly the increases. These panels shows similar results to the panels on the left, but more precisely show the highest increases in the dams on the western coast of the lower peninsula of Michigan., and the highest decreases in the dams on the southern coast of the upper peninsula of Michigan and northeastern Wisconsin.

In particular, dams in the Southern portion of the Lower Peninsula of Michigan face the largest

increase in peak annual discharge, intensifying under each scenario. In the future, great precaution in the form of careful observation and timely maintenance must be taken in order to prevent devastating floods due to dam breaks.

CHAPTER 7

SUMMARY AND CONCLUSION

In summary, the GLB is facing significant changes in hydrology under climate change. Historically, increases in temperature and precipitation have contributed to increases in streamflow over the past 25 years. Similar trends are projected to continue into the future. Overall water balance in the GLB is expected to continue to increase. Over the past 75 years, precipitation over the GLB has increased by 14%. This is reflected by higher river discharge volumes, higher lake water levels and more frequent and intense flooding. Further, the timing of peak flows is expected to come earlier and earlier each year in the coming decades, reflecting higher temperatures and earlier onsets of spring.

In this study, I first examined historical observed streamflow data at USGS gauging stations to determine the impact of dams and climate change on streamflow. Results show that streamflow has increased within the basin throughout the recent decades. This increasing trend is more dominant in the eastern portion of the basin. Next, I examined the impacts of climate change on the hydrology of the GLB throughout the 21st century under 3 climate change scenarios, SSP1, SSP3 and SSP5. Climate change is anticipated to significantly influence the timing, magnitude, and extremes of hydrological events in the region. My results show alterations in seasonal streamflow patterns were observed, including a notable increase in winter discharge by over 50%, and a consistent decline in peak streamflow in March or April. Surface water storage exhibited a general increase, with SSP1 showing the smallest change and SSP3 and SSP5 indicating the highest increase. Lake water levels were shown to increase under all scenarios, most highly under SSP5. Additionally, the analysis of large hydrological extremes demonstrated an overall increase in mean annual flood depth and the occurrence of extreme floods. These changes have broader implications on the region's agriculture and infrastructure.

For agriculture, changes in planting season flood timing, occurrence, and depth were noted, showing increases in all aspects of flooding throughout the basin, especially in flood plain and coastal areas. Growing season drought frequency revealed a spatial pattern, generally showing

decreased severity in the Northern basin and increased severity in the South. Future work on agriculture should focus on assessing the agricultural impacts of these changes, including their effects on spring floods, summer droughts, alterations in seasonality, planting dates, and crop yields. And use a crop model to examine specific impacts on specific crops. Understanding these intricate interactions is crucial for implementing adaptive strategies in agriculture and ensuring the resilience of rural communities in the face of evolving hydrological conditions.

For infrastructure, many dams in the southern portion of the basin saw an increase in peak flows, potentially leading to dam stress and, without proper maintenance and precautions, failure. Future work on infrastructure implications would include more detailed modeling using dam operation schemes, and site specific modeling using HEC-RAS or a similar model. Overall, these results may contain uncertainties caused by the use of a basin-wide model, imperfect model parameterizations, uncertainties in input data, all of which could be improved in future studies. However, this is a pilot study for the use of the CaMa-Flood model in the GLB, and brings into light many important implications of climate change on the GLB. The framework of this study can easily be applied to other works. These results emphasize the complex interactions between climate change and hydrological events in the GLB with implications for water management and infrastructure planning.

BIBLIOGRAPHY

[1] P. E. Abbate, J. L. Dardanelli, M. G. Cantarero, M. Maturano, R. J. M. Melchiori, and E. E. Suero. Climatic and water availability effects on water-use efficiency in wheat. *Crop Science*, 44:474, 2004.

[2] Zurina Z. Abidin, Nur S. Mohd Shamsudin, Norhafizah Madehi, and Shafreeza Sobri. Optimisation of a method to extract the active coagulant agent from jatropha curcas seeds for use in turbidity removal. *Industrial Crops and Products*, 41:319–323, 1 2013.

[3] V A Alexandrov and G Hoogenboom. Vulnerability and adaptation assessments of agricultural crops under climate change in the southeastern usa. *Theoretical and Applied Climatology*, 67:45–63, 2000.

[4] Rawshan Ali, Alban Kuriqi, Shadan Abubaker, and Ozgur Kisi. Long-term trends and seasonality detection of the observed flow in yangtze river using mann-kendall and sen's innovative trend method. *Water (Switzerland)*, 11, 2019.

[5] Yilinuer Alifujiang, Jilili Abuduwaili, and Yongxiao Ge. Trend analysis of annual and seasonal river runoff by using innovative trend analysis with significant test. *Water (Switzerland)*, 13, 2021.

[6] Miguel A. Altieri, Clara I. Nicholls, Alejandro Henao, and Marcos A. Lana. Agroecology and the design of climate change-resilient farming systems, 7 2015.

[7] Ali A. Assani, Raphaëlle Landry, Ouassila Azouaoui, Philippe Massicotte, and Denis Gratton. Comparison of the characteristics (frequency and timing) of drought and wetness indices of annual mean water levels in the five north american great lakes. *Water Resources Management*, 30:359–373, 1 2016.

[8] Mann Henry B. Nonparametric tests against trend author (s): Henry b . mann published by : The econometric society stable url : https://www.jstor.org/stable/1907187 references linked references are available on jstor for this article : You may need to log in to jstor. *Econometrica*, 13:245–259, 1945.

[9] Robert Barr, Laura Bowling, Kyuhyun Byun, Indrajeet Chaubey, Natalie Chin, Darren Ficklin, Alan Hamlet, Stephen Kines, Charlotte Lee, Ram Neupane, Garett Pignotti, Sanoar Rahman, Sarmistha Singh, Pandara Valappil Femeena, and Tanja Williamson. The future of indiana's water resources: A report from the indiana climate change impacts assessment, 6 2023.

[10] Alana M. Bartolai, Lingli He, Ardith E. Hurst, Linda Mortsch, Robert Paehlke, and Donald Scavia. Climate change as a driver of change in the great lakes st. lawrence river basin. *Journal of Great Lakes Research*, 41:45–58, 2015.

[11] Samantha J. Basile, Sara A. Rauscher, and Allison L. Steiner. Projected precipitation changes within the great lakes and western lake erie basin: a multi-model analysis of intensity and seasonality. *International Journal of Climatology*, 37:4864–4879, 11 2017.

[12] F. C. Bell. The areal reduction factor rainfall, frequency estimation. *Institute of Hydrology*, 35, 12 1976.

[13] Frederick C Bell. Not to be reproduced by photoprint or microfilm without written permission from the publisher characteristic response times in design flood estimation, 1969.

[14] L. S. Borma, H. R. Da Rocha, O. M. Cabral, C. Von Randow, E. Collicchio, D. Kurzatkowski, P. J. Brugger, H. Freitas, R. Tannus, L. Oliveira, C. D. Rennó, and P. Artaxo. Atmosphere and hydrological controls of the evapotranspiration over a floodplain forest in the bananal island region, amazonia. *Journal of Geophysical Research: Biogeosciences*, 114, 3 2009.

[15] Laura C. Bowling, Keith A. Cherkauer, Charlotte I. Lee, Janna L. Beckerman, Sylvie Brouder, Jonathan R. Buzan, Otto C. Doering, Jeffrey S. Dukes, Paul D. Ebner, Jane R. Frankenberger, Benjamin M. Gramig, Eileen J. Kladivko, and Jeffrey J. Volenec. Agricultural impacts of climate change in indiana and potential adaptations. *Climatic Change*, 163:2005–2027, 12 2020.

[16] Kyuhyun Byun, Chun Mei Chiu, and Alan F. Hamlet. Effects of 21st century climate change on seasonal flow regimes and hydrologic extremes over the midwest and great lakes region of the us. *Science of the Total Environment*, 650:1261–1277, 2019.

[17] Kyuhyun Byun and Alan F. Hamlet. Projected changes in future climate over the midwest and great lakes region using downscaled cmip5 ensembles. *International Journal of Climatology*, 38:e531–e553, 2018.

[18] Katherine Calvin, Dipak Dasgupta, Gerhard Krinner, Aditi Mukherji, Peter W. Thorne, Christopher Trisos, José Romero, Paulina Aldunce, Ko Barrett, Gabriel Blanco, William W.L. Cheung, Sarah Connors, Fatima Denton, Aïda Diongue-Niang, David Dodman, Matthias Garschagen, Oliver Geden, Bronwyn Hayward, Christopher Jones, Frank Jotzo, Thelma Krug, Rodel Lasco, Yune-Yi Lee, Valérie Masson-Delmotte, Malte Meinshausen, Katja Mintenbeck, Abdalah Mokssit, Friederike E.L. Otto, Minal Pathak, Anna Pirani, Elvira Poloczanska, Hans-Otto Pörtner, Aromar Revi, Debra C. Roberts, Joyashree Roy, Alex C. Ruane, Jim Skea, Priyadarshi R. Shukla, Raphael Slade, Aimée Slangen, Youba Sokona, Anna A. Sörensson, Melinda Tignor, Detlef van Vuuren, Yi-Ming Wei, Harald Winkler, Panmao Zhai, Zinta Zommers, Jean-Charles Hourcade, Francis X. Johnson, Shonali Pachauri, Nicholas P. Simpson, Chandni Singh, Adelle Thomas, Edmond Totin, Andrés Alegría, Kyle Armour, Birgit Bednar-Friedl, Kornelis Blok, Guéladio Cissé, Frank Dentener, Siri Eriksen, Erich Fischer, Gregory Garner, Céline Guivarch, Marjolijn Haasnoot, Gerrit Hansen, Mathias Hauser, Ed Hawkins, Tim Hermans, Robert Kopp, Noëmie Leprince-Ringuet, Jared Lewis, Debora Ley, Chloé Ludden, Leila Niamir, Zebedee Nicholls, Shreya Some, Sophie Szopa, Blair Trewin, Kaj-Ivar van der Wijst, Gundula Winter, Maxim-

ilian Witting, Arlene Birt, and Meeyoung Ha. Ipcc, 2023: Climate change 2023: Synthesis report. contribution of working groups i, ii and iii to the sixth assessment report of the intergovernmental panel on climate change [core writing team, h. lee and j. romero (eds.)]. ipcc, geneva, switzerland., 7 2023.

[19] Maureen Campbell, Matthew J. Cooper, Kathryn Friedman, and William P. Anderson. The economy as a driver of change in the great lakes-st. lawrence river basin. *Journal of Great Lakes Research*, 41:69–83, 2015.

[20] Keith A. Cherkauer and Tushar Sinha. Hydrologic impacts of projected future climate change in the lake michigan region. *Journal of Great Lakes Research*, 36:33–50, 2010.

[21] Keith A. Cherkauer and Tushar Sinha. Hydrologic impacts of projected future climate change in the lake michigan region. *Journal of Great Lakes Research*, 36:33–50, 2010.

[22] Huicheng Chien, Pat J.F. Yeh, and Jason H. Knouft. Modeling the potential impacts of climate change on streamflow in agricultural watersheds of the midwestern united states. *Journal of Hydrology*, 491:73–88, 5 2013.

[23] Tariq A. Deen, M. Altaf Arain, Olivier Champagne, Patricia Chow-Fraser, and Dawn Martin-Hill. Impacts of climate change on streamflow in the mckenzie creek watershed in the great lakes region. *Frontiers in Environmental Science*, 11, 2023.

[24] D. Deryng, W. J. Sacks, C. C. Barford, and N. Ramankutty. Simulating the effects of climate and agricultural management practices on global crop yield. *Global Biogeochemical Cycles*, 25:n/a–n/a, 6 2011.

[25] Hong X. Do, Joeseph P. Smith, Lauren M. Fry, and Andrew D. Gronewold. Seventy-year long record of monthly water balance estimates for earth's largest lake system. *Scientific Data*, 7:1–12, 2020.

[26] Marc D'Orgeville, W. Richard Peltier, Andre R. Erler, and Jonathan Gula. Climate change impacts on great lakes basin precipitation extremes. *Journal of Geophysical Research*, 119:10,799–10,812, 9 2014.

[27] E. Ehsanzadeh, H. M. Saley, T. B.M.J. Ouarda, D. H. Burn, A. Pietroniro, O. Seidou, C. Charron, and D. Lee. Analysis of changes in the great lakes hydro-climatic variables. *Journal of Great Lakes Research*, 39:383–394, 9 2013.

[28] Darren L. Ficklin and Kimberly A. Novick. Historic and projected changes in vapor pressure deficit suggest a continental-scale drying of the united states atmosphere. *Journal of Geophysical Research*, 122:2061–2079, 2 2017.

[29] Scott Fields. Great lakes resources at risk. *Environmental Health Perspectives*, 113:A164–A173, 3 2005.

[30] T. D. Fletcher, H. Andrieu, and P. Hamel. Understanding, management and modelling of urban hydrology and its consequences for receiving waters: A state of the art. *Advances in Water Resources*, 51:261–279, 1 2013.

[31] Javier Fluixá-Sanmartín, Luis Altarejos-García, Adrián Morales-Torres, and Ignacio Escuder-Bueno. Review article: Climate change impacts on dam safety, 9 2018.

[32] Clare M. Goodess. How is the frequency, location and severity of extreme events likely to change up to 2060? *Environmental Science and Policy*, 27:S4–S14, 3 2013.

[33] Andrew D. Gronewold, Vincent Fortin, Brent Lofgren, Anne Clites, Craig A. Stow, and Frank Quinn. Coasts, water levels, and climate change: A great lakes perspective. *Climatic Change*, 120:697–711, 2013.

[34] Andrew D. Gronewold and Craig A. Stow. Unprecedented seasonal water level dynamics on one of the earth's largest lakes. *Bulletin of the American Meteorological Society*, 95:15–17, 2014.

[35] Abhinav Gupta, Rosemary W.H. Carroll, and Sean A. McKenna. Changes in streamflow statistical structure across the united states due to recent climate change. *Journal of Hydrology*, 620, 5 2023.

[36] Hoshin V. Gupta, Harald Kling, Koray K. Yilmaz, and Guillermo F. Martinez. Decomposition of the mean squared error and nse performance criteria: Implications for improving hydrological modelling. *Journal of Hydrology*, 377:80–91, 10 2009.

[37] David Haim, Ralph J. Alig, Andrew J. Plantinga, and Brent Sohngen. Climate change and future land use in the united states: An economic approach. *Climate Change Economics*, 2:27–51, 2 2011.

[38] Mohammad Amin Hariri-Ardebili and Upmanu Lall. Superposed natural hazards and pandemics: Breaking dams, floods, and covid-19, 8 2021.

[39] John Fraser Hart. Part-ownership and farm enlargement in the midwest, 1991.

[40] Holly C Hartmann. Climate change impacts on laurentian great lakes levels l.

[41] J. Huang, J. Halpenny, W. Van Der Wal, C. Klatt, T. S. James, and A. Rivera. Detectability of groundwater storage change within the great lakes water basin using grace. *Journal of Geophysical Research: Solid Earth*, 117, 8 2012.

[42] Thomas G. Huntington. Evidence for intensification of the global water cycle: Review and synthesis. *Journal of Hydrology*, 319:83–95, 3 2006.

[43] Zhenong Jin, Qianlai Zhuang, Jiali Wang, Sotirios V. Archontoulis, Zachary Zobel, and

Veerabhadra R. Kotamarthi. The combined and separate impacts of climate extremes on the current and future us rainfed maize and soybean production under elevated co2. *Global Change Biology*, 23:2687–2704, 7 2017.

[44] Carol A. Johnston and Boris A. Shmagin. Regionalization, seasonality, and trends of streamflow in the us great lakes basin. *Journal of Hydrology*, 362:69–88, 2008.

[45] Scott E. Kalafatis, Maureen Campbell, Frazier Fathers, Katrina L. Laurent, Kathryn B. Friedman, Gail Krantzberg, Don Scavia, and Irena F. Creed. Out of control: How we failed to adapt and suffered the consequences. *Journal of Great Lakes Research*, 41:20–29, 2015.

[46] Krishna Karra, Caitlin Kontgis, Zoe Statman-Weil, Joseph C. Mazzariello, Mark Mathis, and Steven P. Brumby. Global land use/land cover with sentinel 2 and deep learning. In *2021 IEEE International Geoscience and Remote Sensing Symposium IGARSS*, volume 2021-July, pages 4704–4707. Institute of Electrical and Electronics Engineers Inc., 2021.

[47] Gurpreet Kaur, Gurbir Singh, Peter P. Motavalli, Kelly A. Nelson, John M. Orlowski, and Bobby R. Golden. Impacts and management strategies for crop production in waterlogged or flooded soils: A review, 5 2020.

[48] Miraj B. Kayastha, Xinyu Ye, Chenfu Huang, and Pengfei Xue. Future rise of the great lakes water levels under climate change. *Journal of Hydrology*, 612:128205, 9 2022.

[49] M G Kendall. *Rank correlation methods.* Griffin, 1948.

[50] John M. Kerr, Joseph V. DePinto, Dennis McGrath, Scott P. Sowa, and Scott M. Swinton. Sustainable management of great lakes watersheds dominated by agricultural land use. *Journal of Great Lakes Research*, 42:1252–1259, 12 2016.

[51] R. Killick, P. Fearnhead, and I. A. Eckley. Optimal detection of changepoints with a linear computational cost. *Journal of the American Statistical Association*, 107:1590–1598, 2012.

[52] Julian Kirchherr and Katrina J. Charles. The social impacts of dams: A new framework for scholarly analysis. *Environmental Impact Assessment Review*, 60:99–114, 9 2016.

[53] Heidi Kreibich, Anne F. Van Loon, Kai Schröter, Philip J. Ward, Maurizio Mazzoleni, Nivedita Sairam, Guta Wakbulcho Abeshu, Svetlana Agafonova, Amir AghaKouchak, Hafzullah Aksoy, Camila Alvarez-Garreton, Blanca Aznar, Laila Balkhi, Marlies H. Barendrecht, Sylvain Biancamaria, Liduin Bos-Burgering, Chris Bradley, Yus Budiyono, Wouter Buytaert, Lucinda Capewell, Hayley Carlson, Yonca Cavus, Anaïs Couasnon, Gemma Coxon, Ioannis Daliakopoulos, Marleen C. de Ruiter, Claire Delus, Mathilde Erfurt, Giuseppe Esposito, Didier François, Frédéric Frappart, Jim Freer, Natalia Frolova, Animesh K. Gain, Manolis Grillakis, Jordi Oriol Grima, Diego A. Guzmán, Laurie S. Huning, Monica Ionita, Maxim Kharlamov, Dao Nguyen Khoi, Natalie Kieboom, Maria Kireeva, Aristeidis Koutroulis, Waldo Lavado-Casimiro, Hong Yi Li, María Carmen LLasat, David

Macdonald, Johanna Mård, Hannah Mathew-Richards, Andrew McKenzie, Alfonso Mejia, Eduardo Mario Mendiondo, Marjolein Mens, Shifteh Mobini, Guilherme Samprogna Mohor, Viorica Nagavciuc, Thanh Ngo-Duc, Thi Thao Nguyen Huynh, Pham Thi Thao Nhi, Olga Petrucci, Hong Quan Nguyen, Pere Quintana-Seguí, Saman Razavi, Elena Ridolfi, Jannik Riegel, Md Shibly Sadik, Elisa Savelli, Alexey Sazonov, Sanjib Sharma, Johanna Sörensen, Felipe Augusto Arguello Souza, Kerstin Stahl, Max Steinhausen, Michael Stoelzle, Wiwiana Szalińska, Qiuhong Tang, Fuqiang Tian, Tamara Tokarczyk, Carolina Tovar, Thi Van Thu Tran, Marjolein H.J. Van Huijgevoort, Michelle T.H. van Vliet, Sergiy Vorogushyn, Thorsten Wagener, Yueling Wang, Doris E. Wendt, Elliot Wickham, Long Yang, Mauricio Zambrano-Bigiarini, Günter Blöschl, and Giuliano Di Baldassarre. The challenge of unprecedented floods and droughts in risk management. *Nature*, 608:80–86, 8 2022.

[54] Naveen Kumar, Arvind Kumar, Binny Mary Marwein, Daneshver Kumar Verma, Binny Marry Marwein, Ilakiya Jayabalan, Agam Kumar, and Duraisamy Ramamoorthy. Agricultural activities causing water pollution and its mitigation-a review. *International Journal of Modern Agriculture*, 10, 2021.

[55] Kenneth E. Kunkel, David R. Easterling, Kenneth Hubbard, and Kelly Redmond. Temporal variations in frost-free season in the united states: 1895-2000. *Geophysical Research Letters*, 31, 2 2004.

[56] Stefan Lange. Isimip3b bias adjustment fact sheet, 2021.

[57] Guoyong Leng and Maoyi Huang. Crop yield response to climate change varies with crop spatial distribution pattern. *Scientific Reports*, 7, 12 2017.

[58] Guoyong Leng, Xuesong Zhang, Maoyi Huang, Ghassem R. Asrar, and L. Ruby Leung. The role of climate covariability on crop yields in the conterminous united states. *Scientific Reports*, 6, 9 2016.

[59] GU LIANHONG, PAUL J. HANSON, W. MAC POST, DALE P. KAISER, BAI YANG, RAMAKRISHNA NEMANI, STEPHEN G. PALLARDY, and TILDEN MEYERS. The 2007 eastern us spring freeze: Increased cold damage in a warming world? *BioScience*, 58:253–262, 2008.

[60] Xiajing Lin, Guohe Huang, Joseph M. Piwowar, Xiong Zhou, and Yuanyuan Zhai. Risk of hydrological failure under the compound effects of instant flow and precipitation peaks under climate change: A case study of mountain island dam, north carolina. *Journal of Cleaner Production*, 284, 2 2021.

[61] Geoffrey Linkemer, James E. Board, and Mary E. Musgrave. Waterlogging effects on growth and yield components in late-planted soybean. *Crop Science*, 38:1576–1584, 1998.

[62] David B. Lobell. Climate change adaptation in crop production: Beware of illusions, 2014.

[63] David B. Lobell, Kenneth G. Cassman, and Christopher B. Field. Crop yield gaps: Their importance, magnitudes, and causes. *Annual Review of Environment and Resources*, 34:179–204, 2009.

[64] Elena Loreti, Hans van Veen, and Pierdomenico Perata. Plant responses to flooding stress, 10 2016.

[65] Charles H Luce, Katie D Newcomb, Robert W Hoyer, Joseph H Blanchard, and Jessica E Halofsky. Chapter 3 : Climate change effects on water resources and infrastructure in southwest oregon, 2018.

[66] Edouard Mailhot, Biljana Music, Daniel F. Nadeau, Anne Frigon, and Richard Turcotte. Assessment of the laurentian great lakes' hydrological conditions in a changing climate. *Climatic Change*, 157:243–259, 11 2019.

[67] Elizabeth Marshall, Marcel Aillery, Scott Malcolm, and Ryan Williams. Agricultural production under climate change: The potential impacts of shifting regional water balances in the united states. *American Journal of Agricultural Economics*, 97:568–588, 3 2015.

[68] E Mcbean and H Motiee. Hydrology and earth system sciences assessment of impact of climate change on water resources: a long term analysis of the great lakes of north america, 2008.

[69] Linda Mortsch, Henry Hengeveld, Murray Lister, Brent Lofgren, Frank Quinn, Michel Slivitzky, and Lisa Wenger. Climate change impacts on the hydrology of the great lakes-st. lawrence system. *Canadian Water Resources Journal*, 25:153–179, 2000.

[70] I. Nalbantis and G. Tsakiris. Assessment of hydrological drought revisited. *Water Resources Management*, 23:881–897, 2009.

[71] Bibi S. Naz, Shih Chieh Kao, Moetasim Ashfaq, Huilin Gao, Deeksha Rastogi, and Sudershan Gangrade. Effects of climate change on streamflow extremes and implications for reservoir inflow in the united states. *Journal of Hydrology*, 556:359–370, 1 2018.

[72] M. L. (Martin L.) Parry and Intergovernmental Panel on Climate Change. Working Group II. *Climate change 2007 : impacts, adaptation and vulnerability : contribution of Working Group II to the fourth assessment report of the Intergovernmental Panel on Climate Change*. Cambridge University Press, 2007.

[73] Elisha Persaud, Jana Levison, Scott MacRitchie, Steven J. Berg, Andre R. Erler, Beth Parker, and Edward Sudicky. Integrated modelling to assess climate change impacts on groundwater and surface water in the great lakes basin using diverse climate forcing. *Journal of Hydrology*, 584, 5 2020.

[74] Karen R. Ryberg, Glenn A. Hodgkins, and Robert W. Dudley. Change points in annual peak

streamflows: Method comparisons and historical change points in the united states. *Journal of Hydrology*, 583:124307, 2020.

[75] Karen R. Ryberg, Glenn A. Hodgkins, and Robert W. Dudley. Change points in annual peak streamflows: Method comparisons and historical change points in the united states. *Journal of Hydrology*, 583:124307, 2020.

[76] Somayeh Salehi, Majid Dehghani, Sayed M. Mortazavi, and Vijay P. Singh. Trend analysis and change point detection of seasonal and annual precipitation in iran. *International Journal of Climatology*, 40:308–323, 2020.

[77] Wolfram Schlenker and Michael J Roberts. Nonlinear temperature effects indicate severe damages to u.s. crop yields under climate change, 2009.

[78] Aleix Serrat-Capdevila, Russell L. Scott, W. James Shuttleworth, and Juan B. Valdés. Estimating evapotranspiration under warmer climates: Insights from a semi-arid riparian system. *Journal of Hydrology*, 399:1–11, 3 2011.

[79] Narayan K. Shrestha, Frank Seglenieks, André G.T. Temgoua, and Armin Dehghan. The impacts of climate change on land hydroclimatology of the laurentian great lakes basin. *Frontiers in Water*, 4, 7 2022.

[80] Sabin Shrestha, Suresh Sharma, Rishabh Gupta, and Rabin Bhattarai. Impact of global climate change on stream low flows: A case study of the great miami river watershed, ohio. *International Journal of Agricultural and Biological Engineering*, 12:84–95, 2019.

[81] Cuihong Song, Kevin H. Gardner, Sharon J.W. Klein, Simone Pereira Souza, and Weiwei Mo. Cradle-to-grave greenhouse gas emissions from dams in the united states of america, 7 2018.

[82] Jane Southworth, J C Randolph, M Habeck, O C Doering, R A Pfeifer, D G Rao, and J J Johnston. Consequences of future climate change and changing climate variability on maize yields in the midwestern united states, 2000.

[83] Mark G. Stewart, Xiaoming Wang, and Minh N. Nguyen. Climate change adaptation for corrosion control of concrete infrastructure. *Structural Safety*, 35:29–39, 2012.

[84] Zachary J. Suriano. On the role of snow cover ablation variability and synoptic-scale atmospheric forcings at the sub-basin scale within the great lakes watershed. *Theoretical and Applied Climatology*, 135:607–621, 1 2019.

[85] Hossein Tabari. Climate change impact on flood and extreme precipitation increases with water availability. *Scientific Reports*, 10, 12 2020.

[86] Kassa Abera Tareke and Admasu Gebeyehu Awoke. Hydrological drought analysis using

streamflow drought index (sdi) in ethiopia. *Advances in Meteorology*, 2022, 2022.

[87] Karl E. Taylor. Summarizing multiple aspects of model performance in a single diagram. *Journal of Geophysical Research Atmospheres*, 106:7183–7192, 4 2001.

[88] Ethan J. Theuerkauf and Katherine N. Braun. Rapid water level rise drives unprecedented coastal habitat loss along the great lakes of north america. *Journal of Great Lakes Research*, 47:945–954, 8 2021.

[89] Kevin E Trenberth. The impact of climate change and variability on heavy precipitation, floods, and droughts, 2005.

[90] Gachomo Dorcas Wambui. The power of the pruned exact linear time(pelt) test in multiple changepoint detection. *American Journal of Theoretical and Applied Statistics*, 4:581, 2015.

[91] Jin Wang, Sai Kranthi Vanga, Rachit Saxena, Valérie Orsat, and Vijaya Raghavan. Effect of climate change on the yield of cereal crops: A review, 6 2018.

[92] Lihong Wang, Shenghui Cui, Yuanzheng Li, Hongjie Huang, Bikram Manandhar, Vilas Nitivattananon, Xuejuan Fang, and Wei Huang. A review of the flood management: from flood control to flood resilience, 11 2022.

[93] Lili Wang, Keith A. Cherkauer, and Dennis C. Flanagan. Impacts of climate change on soil erosion in the great lakes region. *Water (Switzerland)*, 10, 6 2018.

[94] L. Warszawski. Isimip3a simulation data from the global water sector, 2024.

[95] L. Warszawski. Isimip3b simulation data from the global water sector, 2024.

[96] Lila Warszawski, Katja Frieler, Veronika Huber, Franziska Piontek, Olivia Serdeczny, and Jacob Schewe. The inter-sectoral impact model intercomparison project (isi–mip): Project framework. *Proceedings of the National Academy of Sciences*, 111(9):3228–3232, December 2013.

[97] Rodney E. Will, Stuart M. Wilson, Chris B. Zou, and Thomas C. Hennessey. Increased vapor pressure deficit due to higher temperature leads to greater transpiration and faster mortality during drought for tree seedlings common to the forest-grassland ecotone. *New Phytologist*, 200:366–374, 10 2013.

[98] Dai Yamazaki, Shinjiro Kanae, Hyungjun Kim, and Taikan Oki. A physically based description of floodplain inundation dynamics in a global river routing model. *Water Resources Research*, 47:1–21, 2011. Introducing CaMa-Flood model!

This model uses small-scale topography. rather than global models (can regionalize - crop map)

The model can examine topography- based on 1 km resolution DEM- within a grid, and examine the relationship between water storage, level, and flooded area in the model

Water

transportation among cells is calculated using wave equation

Results: improved prediction of river discharge, water surface elevation, and inundated areas.

[99] Mengqi Zhao and Jan Boll. Adaptation of water resources management under climate change.

[100] Samuel C. Zipper, Jiangxiao Qiu, and Christopher J. Kucharik. Drought effects on us maize and soybean production: Spatiotemporal patterns and historical changes. *Environmental Research Letters*, 11, 9 2016.